Aus der Klinik für Neurologie mit experimenteller Neurologie
der Medizinischen Fakultät Charité – Universitätsmedizin Berlin

DISSERTATION

Mechanisms triggering spreading depolarizations in a mouse model of acute and subacute cortical hemorrhage

Entstehungsmechanismen von Spreading Depolarizations in einem Mausmodell akuter und subakuter kortikaler Blutungen

zur Erlangung des akademischen Grades
Medical Doctor - Doctor of Philosophy (MD/PhD)

vorgelegt der Medizinischen Fakultät
Charité – Universitätsmedizin Berlin

von

Paul Fischer

aus Berlin

Datum der Promotion: 30.11.2023

Table of Contents

List of figures

Abbreviations

ANOVA	Analysis of variance
ARRIVE	Animal Research: Reporting of In Vivo Experiments
BBB	Blood-brain barrier
BP	Blood pressure
CAA	Cerebral amyloid angiopathy
Ca^{2+}	Calcium
CBF	Cerebral blood flow
CO_2	Carbon dioxide
COSBID	Co-Operative Studies on Brain Injury Depolarizations
DC	Direct current
dMCAo	Distal Middle Cerebral Artery occlusion
ECoG	Electrocorticogram
Hb	Hemoglobin
ICH	Intracerebral hemorrhage
iHTN	Induced hypertension
IOS	Intrinsic optical signal
IU	International unit
K^+	Potassium
KCl	Potassium chloride
LSF	Laser speckle flowmetry
MCA	Middle Cerebral Artery
N_2	Nitrogen
Na^+	Sodium
NaCl	Sodium chloride
Na^+,K^+-ATPase	Sodium,potassium-adenosine triphosphatase

NBO	Normobaric hyperoxia
NIH	National Institutes of Health
O_2	Oxygen
$paCO_2$	Partial arterial pressure of carbon dioxide
paO_2	Partial arterial pressure of oxygen
PBS	Phosphate-buffered saline
ROI	Region of interest
SAH	Subarachnoid hemorrhage
SD	Spreading depolarization

Abstract

Background: Spreading depolarizations (SDs) are waves neuronal and glial mass-depolarization that occur spontaneously after brain injury and are associated with detrimental effects in ischemic stroke and subarachnoid hemorrhage. In clinical and experimental intracerebral hemorrhage (ICH), SDs are observed. However, triggers for SD in ICH are poorly understood. In a mouse model, we investigated spatiotemporal characteristics and causes of SD occurrence in acute and subacute stages of ICH. We focused on ischemia, mechanical tissue distortion, and blood constituents or blood breakdown products as potential triggers.

Methods: After cannulating the femoral artery to track systemic physiology, ICH was induced by cortical injection of bacterial collagenase VII-S. Immediately, 8h, 24h, or 48h after injection, intrinsic optical signals, laser speckle flowmetry (LSF), and electrocorticography were recorded for 240 min to follow hematoma expansion, cortical blood flow changes, and SD occurrence over time. Subgroups of animals were assigned to normobaric hyperoxia or induced hypertension in the early stages of ICH. In another subset of animals, focal cortical ischemia was induced instead of ICH using the distal Middle Cerebral Artery occlusion model (dMCAo). Brains were collected at the end of the experiment for tissue analysis.

Results: During acute stages of ICH (0–4h), 45% of mice developed SDs, that often occurred in couplets and invariably emerged from the hematoma. SD frequency observed in primary hemorrhagic lesions was three-fold lower than in size-matched ischemic cortical infarcts. Arguing against blood constituents or breakdown products as a trigger for SD in ICH, hematoma size did not correlate with SD occurrence. Further, SDs were only detected 29 to 221 min after ICH induction, whereas not a single SD was recorded at later time points, 8–52h after ICH induction. Likely excluding ischemia as a potential trigger, perihematomal perfusion monitored using LSF did not predict SD occurrence. In line with this, normobaric hyperoxia, known to decrease SD frequency by 60% in focal ischemic brains, did not reduce SD occurrence. Instead, SDs always arose during phases of rapid hemorrhage growth, which was doubled immediately preceding an SD, compared with the peak growth recorded in animals that did not develop any SD. Inducing hypertension

in a separate cohort of mice yielded severely accelerated hemorrhage growth and increased SD frequency by four-fold compared with normotensive controls.

Conclusion: Our data provide novel mechanistic insights into the origins of SDs in ICH. They suggest that spontaneous SDs are caused by the mechanical tissue distortion of rapidly growing hematomas, with ischemia and blood constituents or breakdown products not contributing to a relevant extent.

Zusammenfassung

Hintergrund: Spreading depolarizations (SDs) sind Wellen neuronaler und glialer Massen-Depolarisation, die spontan nach Hirnverletzungen auftreten und mit schädlichen Effekten bei ischämischen Schlaganfällen und Subarachnoidalblutungen in Verbindung gebracht werden. Sie können im Rahmen klinischer und experimenteller intrazerebraler Blutungen (ICH) beobachtet werden. Ihre Auslöser hier sind jedoch unbekannt.
In einem Mausmodell analysierten wir das Auftreten und die Ursachen von SDs in akuten und subakuten ICH-Stadien und untersuchten Ischämie, mechanische Gewebsverdrängung und Blutbestandteile oder -abbauprodukte als mögliche Auslöser.

Methodik: Nach Kanülierung der Femoralarterie zur Überwachung der systemischen Physiologie wurde durch kortikale Injektion von bakterieller Kollagenase VII-S eine ICH induziert. Unmittelbar, 8h, 24h, oder 48h nach der Injektion wurden intrinsische optische Signale, Laser-Speckle-Flussmessung (LSF) und Elektrokortikographie 240 min lang aufgezeichnet, um die Ausdehnung der Blutung, Veränderungen des kortikalen Blutflusses und das Auftreten von SDs im Zeitverlauf zu beurteilen. Untergruppen von Tieren wurden im Frühstadium der ICH einer normobaren Hyperoxie oder einer induzierten Hypertension unterzogen. In einer anderen Subgruppe wurde anstelle der ICH mit Hilfe des dMCAo Modells eine fokale Ischämie induziert. Am Ende der Experimente wurden die Gehirne zur Gewebsanalyse entnommen.

Ergebnisse: In der akuten Phase der ICH (0-4h) entwickelten 45 % der Mäuse SDs, die oft in Paaren auftraten und ausnahmslos von der Blutung ausgingen. Primär hämorrhagische kortikale Läsionen zeigten eine, im Vergleich zu gleich großen kortikalen ischämischen Infarkten, um das dreifach reduzierte SD-Frequenz.
SDs traten lediglich 29 bis 221min nach ICH-Induktion auf, nicht jedoch später, 8-52h nach ICH-Induktion, und korrelierten in ihrem Auftreten nicht mit der Blutungsgröße, was gegen Blutbestandteile oder Abbauprodukte als Auslöser der SDs sprach. Weiterhin konnte der peri-hämatomale Blutfluss das Erscheinen von SDs nicht vorhersagen und auch normobare Hyperoxie, die das Vorkommen von SDs in fokal ischämischen Gehirnen um 60 % reduziert, beeinflusste die SD-Frequenz nicht. Dies machte eine fokale Ischämie als Auslöser der SDs ebenso unwahrscheinlich. Im Gegensatz dazu zeigte sich, dass SDs immer in Phasen starken Blutungswachstums auftraten, das unmittelbar vor dem Erscheinen einer SD doppelt so hoch war wie das maximale Blutungswachstum in Tieren, die keine SDs entwickelten. Verglichen mit normotensiven Tieren führte induzierte Hypertension zu einem stark beschleunigtem Blutungswachstum und einer Vervierfachung der SD-Frequenz.

Zusammenfassung: Unsere Daten liefern neue pathophysiologische Erkenntnisse zur Entstehung von SDs bei ICH. Sie legen nahe, dass SDs durch mechanischen Druck schnell wachsender Blutungen ausgelöst werden, während Ischämie und Blutbestandteile, oder -abbauprodukte das Auftreten von SDs nicht relevant beeinflussen.

1 Introduction

1.1 Mechanisms of intracerebral hemorrhage

Intracerebral hemorrhage (ICH) accounts for 7-28% of worldwide strokes[1-4] and has particularly high incidence rates in lower- and middle-income countries, especially in Oceania, Central, East, and Southeast Asia[3]. It is a devastating type of acute brain injury with a case fatality of up to 50% after one month and more than 70% after five years[5] that did not change in the recent past[2, 5-8]. Amongst all neurological diseases, ICH holds one of the largest burdens of disability-adjusted life years[3], as up to 80% of surviving patients fail to regain pre-morbid levels of functional independence[9, 10].

Characterized by bleeding from a ruptured cerebral vessel, often into ganglionic, lobar, cerebellar, and pontine brain parenchyma[11], the majority of spontaneous ICH originates from primary pathoetiologies. These include hypertension (~65%)[10, 12], and cerebral amyloid angiopathy (CAA)[10], a disease of small arteries and arterioles in which deposition of β-Amyloid or other amyloid proteins damages the vessel wall[13]. Fewer cases can be attributed to secondary causes, which include brain tumors, aneurysms, arteriovenous malformations, and hemorrhagic conversion of ischemic stroke [14, 15]. Moreover, a third etiologic group of up to 20% of ICH cases has recently evolved that occurs in the context of pharmacologically induced coagulopathy[16]. This third group likely emerged due to increased use of antithrombotic medication and might explain unchanged ICH incidence in high-income countries within the last decades despite improved hypertension management[17].

Upon initial vessel rupture an injury cascade is triggered that can be divided into primary and secondary injury. The primary injury occurs immediately after ICH onset within the first days and is caused by the mass effect of the hematoma, hematoma expansion, increased intracranial pressure, and the impact of hydrocephalus[14, 15]. Causing local physical disruption of brain tissue, mechanisms of primary injury can lead to midline shift and herniation, resulting in more widespread mechanical injury[15]. Nevertheless, a reduction of cerebral blood flow (CBF) due to vessel rupture and the mass effect of the hematoma does not result in ischemic conditions, at least in larger amounts of brain tissue[18-24]. The

secondary injury develops several days to weeks after the initial bleeding event via downstream pathways. It is related to inflammation, oxidative stress, iron- and blood-related toxicity, as well as perihematomal edema formation[14, 15].

Further knowledge on ICH's complex injury mechanisms seems crucial in order to improve clinical outcomes as there is still not a single pharmacological treatment that has been shown to improve neurological outcomes or survival after ICH[15, 25, 26].

1.2 Mechanisms of spreading depolarization

Spreading depolarization (SD) is a wave of sudden intense neuronal and glial mass-depolarization that propagates slowly with a speed of approximately 2-8 mm/min in the gray matter of the brain[27-29]. First described by Aristides Leão in 1944[30], it has been observed in insects[31], fish[32], and reptiles[33], as well as in the brain of mammals like the lissencephalic mouse[29, 34], the gyrencephalic swine[35-37], and humans[38-48]. Therefore, SD is considered a species-independent neurologic phenomenon involved in fundamental processes of brain physiology.

To best capture the nature of SD, electrophysiologic, metabolic, and hemodynamic features have to be considered, amongst others. During an SD, first, yet unidentified large conductance, non-selective cation channels open and cause an almost complete breakdown of ion gradients with a pronounced rise of extracellular K^+ and intracellular Na^+ and Ca^{2+} concentrations[28, 49]. Large-scale shifts in concentrations of a multitude of neurotransmitters, metabolites, and small molecules, including glutamate[27], are also observed. Further, neuronal swelling and dendritic blebbing occur as water follows the altered osmotic gradients[50].

While the described changes last up to a minute, markedly increased K^+ and glutamate concentrations in the extracellular space are then thought to diffuse to adjacent neurons and might contribute to triggering the same depolarization and associated ion shifts resulting in a wave-like spread of depolarization in adjacent brain tissue independent of vascular terretories[51, 52]. Importantly, this propagation of SD is limited to brain structures with high neuronal and synaptic density, i.e., gray matter, because the pronounced elevation in K^+ and glutamate concentrations is considered requisite for wave spread. However, SD propagation's exact mechanisms still need to be fully understood[52].

In grey matter structures, the depolarization itself and the massive metabolic shifts accompanying an SD trigger a complex multiphasic vasomotor reaction that differs between various species[34]. Briefly, a simplified prototypical hemodynamic response consisting of four phases can be depicted[34]. First, a phase of transient hypoperfusion or vasoconstriction is observed during tissue depolarization. This is immediately followed by a second hyperemic phase that lasts a couple of minutes while repolarization takes place. After a variable late increase in CBF lasting for a few minutes, a prolonged oligemia is induced that can last for more than an hour[34].

The almost total loss of membrane potential during an SD results in the suppression of action potentials and synaptic activity for approximately one minute, which is depicted in a depression of the electrocorticogram (ECoG) first described by Aristides Leão in 1944[30]. Ionic and water shifts further generate an SD-specific extracellular negative slow potential shift (DC shift)[53] that can be used to monitor SDs experimentally. Based on the characteristic electrophysiologic footprint, in clinical and experimental settings, single SDs, but also couplets of two consecutive SDs or clusters of multiple SDs, can be observed.

To spark an SD, a minimum critical amount of brain tissue, approximately 1 mm^3, has to be depolarized simultaneously[54] by specific triggers that can be divided into two main groups. The first group contains triggers that depolarize neurons by Na^+ or Ca^{2+}-channel activation, like ictal epileptic events or K^+. The second group includes conditions like hypoglycemia, hypoxia, and ischemia that trigger SD depolarizing neurons indirectly by sodium, potassium-adenosine triphosphatase (Na^+,K^+-ATPase) activity reduction[27]. Mechanical stimulation or trauma is known to trigger SD, too. In fact, SD occurs not only after trauma but in various experimental models of brain injury. Research in mouse models has shown that in focal cerebral ischemia, recurrent SDs are triggered when resting state supply-demand mismatch in ischemic penumbra is temporarily aggravated by reduced supply or increased demand, for example, due to functional activation[55]. In subarachnoid hemorrhage (SAH), SDs may be triggered due to secondary cerebral ischemia or mechanical pressure effect[56, 57]. Moreover, whether constituents or breakdown products of focally accumulated blood cause SDs, has been discussed controversially, particularly in the context of SAH[56-58]. As mentioned above, the blood constituent and excitatory amino acid glutamate is believed to at least contribute to triggering the SD wave spread. Further, the synergistic effects of blood breakdown products K^+, a highly potent trigger for SD[56], and the nitric oxide (NO) scavenger Hemoglobin (Hb) have been a center of this

discussion[56, 59, 60]. This is because a decline in NO results in a distinct reduction of the K^+ threshold that has to be reached to trigger SD[61].

1.3 Spreading depolarizations in intracerebral hemorrhage

Historically, the need for invasive electrophysiological monitoring in the form of subdural or intracortical recordings has made SD a clinically under-investigated phenomenon in neurological disease. Just about 20 years ago, SDs were first documented in the context of brain injury in humans[46]. Due to tremendous efforts of the Co-Operative Studies on Brain Injury Depolarizations (COSBID) network and others, 80 years after the initial description of SDs by Leão[30], it is now known that SDs occur for hours and sometimes days after brain injury in more than 50% of patients suffering from traumatic brain injury[40, 41], 70-80% with subarachnoid hemorrhage[38, 39] and almost every patient with malignant hemispheric ischemic stroke[48, 62]. First monitored in a patient after spontaneous ICH in 2002 by Strong et al.[46], over the past two decades, multiple studies have confirmed the existence of SD in patients suffering from ICH, as well[40, 42, 44-46]. Following initial studies with relatively low numbers of patients, often in mixed cohorts of various brain injuries, Helbok et al. recently detected SDs in 18 out of 27 ICH patients[42]. Of note, in none of the existing studies, recordings were started earlier than multiple hours after ICH onset limiting the findings to subacute phases of ICH in which peak SD incidence was reported on day two after ictus[42].

Despite the striking evidence of SD occurrence in the majority of patients suffering from ICH, only a few studies have investigated SD in experimental ICH[35-37]. These three studies focused on the complex spatial and temporal characteristics of SD occurrence and propagation in the gyrencephalic swine brain. They detected SD as early as 17 minutes[36], 38 minutes[35], or 105 minutes[37] after hemorrhage induction, while further SDs could be observed for multiple hours in imaging periods of up to 19h[35-37]. Albeit in a relatively invasive setting, as craniotomy had to be performed to place subdural electrodes for electrophysiologic recordings, these studies demonstrated SD occurrence in both acute and subacute phases of ICH and arguably paved the path for further research examining SD in ICH. Yet, for almost ten years, SD has not been investigated in experimental models of ICH.

1.4 Objectives

Considering the various neurophysiologic alterations associated with SD, it seems essential to notice that the metabolic and hemodynamic response to SD does not deal damage to otherwise healthy tissue. In fact, the reversible neurologic symptoms characteristic of migraine aura are widely believed to reflect spreading depolarization propagating the brain[28]. However, under metabolically compromised conditions, SD can have deleterious consequences. In the context of reduced cerebral perfusion pressure, for example, an inverse hemodynamic response can be observed, which is dominated by profound vasoconstriction, further worsening supply-demand-mismatch in tissue already at risk for irreversible neuronal injury[28, 29, 34]. Moreover, SD can disrupt the blood-brain barrier (BBB) by upregulating matrix metalloproteinase-9[63] and has further been proven to activate inflammatory cascades[64-68]. Thus, SD is considered a mechanism for acute and subacute injury progression of ischemic stroke[28, 55, 62, 69, 70] and SAH[47, 59, 60, 71-75].

Detected in a majority of patients, SD plays a highly underappreciated role in the pathophysiology of ICH, considering the widely suggested deleterious role of SD in other brain injuries. Nevertheless, to date, the mechanisms underlying SD occurrence in ICH are poorly understood. Interestingly, multiple common triggers for SD in other brain injuries could evoke SD in ICH, too. Those triggers include anoxic or ischemic failure of Na^+,K^+-ATPase potentially resulting from vessel rupture or tissue distortion, exposure to blood constituents, or breakdown products resulting from extravasated blood or mechanical tissue distortion caused by the growing hematoma.

Here, we undertook a comprehensive investigation of spatial and temporal characteristics of SD occurrence in a minimally invasive mouse model of acute and subacute ICH and examined potential mechanisms triggering SDs.

The research questions and hypotheses addressed in the following sections are:

1. What are the spatial and temporal characteristics of SD occurrence in acute or subacute phases of cortical hemorrhage in the mouse?
2. What triggers SD in acute or subacute phases of cortical hemorrhage in the mouse?
   a) Blood constituents or breakdown products trigger SD in cortical hemorrhage.
   b) Focal ischemia triggers SD in cortical hemorrhage.
   c) Mechanical tissue distortion triggers SD in cortical hemorrhage.

2 Methods

2.1 Experimental animals

Experimental procedures were approved by the Massachusetts General Hospital Institutional Animal Care and Use Committees following the NIH Guide for Use and Care of Laboratory Animals. A total of 89 male and 13 female CD1 mice (3.7 ± 2.1 months; 36.8 ± 5.5 grams; Charles River Laboratories, Wilmington, MA, USA) were housed in groups of up to 5 animals at a 12-hour light/dark cycle (light exposure from 7 a.m. to 7 p.m.). Room temperature was set to approximately 25 °C with an air humidity of 45-65%. Mice were allowed food and tap water ad libitum.

In control groups, no sex-related differences could be observed. Therefore, data from male and female animals were pooled.

2.2 General surgical preparation

Mice were anesthetized using isoflurane (2.5% induction, 1 – 1.25% maintenance) in 70% N_2 and 30% O_2 throughout the experiment and allowed to breathe spontaneously. Body temperature was monitored via a rectal probe and kept at 37 ± 0.3 °C using a heating pad (TC-1000 Temperature Controller, CWE, Ardmore, PA, USA). To measure parameters of systemic physiology, first, the left femoral artery was catheterized. Blood pressure (BP) and heart rate were then tracked continuously via an arterial cannula connected to a 0.9% NaCl-filled tube that transmitted the blood pressure wave to a transducer (PowerLab; ADInstruments, Colorado Springs, MO, USA). Blood samples of 25 µl were taken from the arterial tube 120 min and 240 min after hemorrhage induction to measure arterial pH, $paCO_2$, and paO_2.

After femoral artery cannulation, animals were placed in a stereotactic frame for surgical preparation. Local anesthetic (Lidocaine gel 2%) was applied onto the scalp and the skull exposed by incising the scalp over the midline. Connective tissue was carefully removed. To prevent the skull from drying and maintain skull translucency, mineral oil was repeatedly applied every 30 minutes for the remainder of the experiment. Baseline images were

recorded for laser speckle flowmetry (LSF) to monitor CBF, and intrinsic optical signal (IOS), to detect SDs, as explained in detail later.

Under saline cooling, two boreholes were drilled over the right hemisphere of the brain to monitor SDs by characteristic changes of extracellular steady potential recordings at a distant frontal side (1.5 mm anterior and 0.5 mm lateral to the bregma) or induce a strictly cortical hemorrhage (2 mm posterior and 3 mm lateral from bregma)[76]. Thereafter, animals were allowed to stabilize for 20 min. A glass capillary microelectrode (tip diameter ~10 µm) was then connected to a differential amplifier (EX1; Dagan Corporation, Minneapolis, MN, USA), along with an analog to digital converter (PowerLab; ADInstruments, Colorado Springs, CO, USA), filled with 0.9% NaCl and slowly inserted 300 µm deep into the cortex through the anterior borehole. The absence of SDs during drilling and electrode insertion was confirmed via LSF and IOS imaging. After general surgical preparation, cortical hemorrhage was induced. The experimental setup is shown in Figure 1A.

2.3 Cortical hemorrhage model and hemorrhage induction

In our study, we aimed to induce an ICH strictly limited to the cortex. Even though SD not only occurs in cortical brain tissue but also in other gray matter structures like the striatum upon injury[77], only a cortical hemorrhage allowed for the imaging we intended using IOS and LSF coupled to electrophysiologic measurements.

A tailor-made protocol was developed in which the depth and area of injection, as well as the amount and dilution of bacterial collagenase VII-S, were adjusted from the existing mouse model of striatal ICH induced by collagenase VII-S. In the striatal ICH model bacterial collagenase is injected to break down the basal lamina of multiple various vessels, yielding spontaneous hemorrhage[25, 78]. Experimental ICH induction by collagenase VII-S is thought to convincingly mimic clinical ICH, especially due to its spontaneous hemorrhage[78, 79]. It has been one of the most widely used models of experimental ICH since its introduction in the 90s[80] due to its simplicity, consistency, and dose-dependent hemorrhage volume[78].

First, the optimal injection parameters were investigated in pilot experiments. The depth of injection was set to 0.5 mm, equidistant from the cortical surface and the corpus callosum, to allow the hemorrhage to grow to the surface and into depth. Similarly, the injection

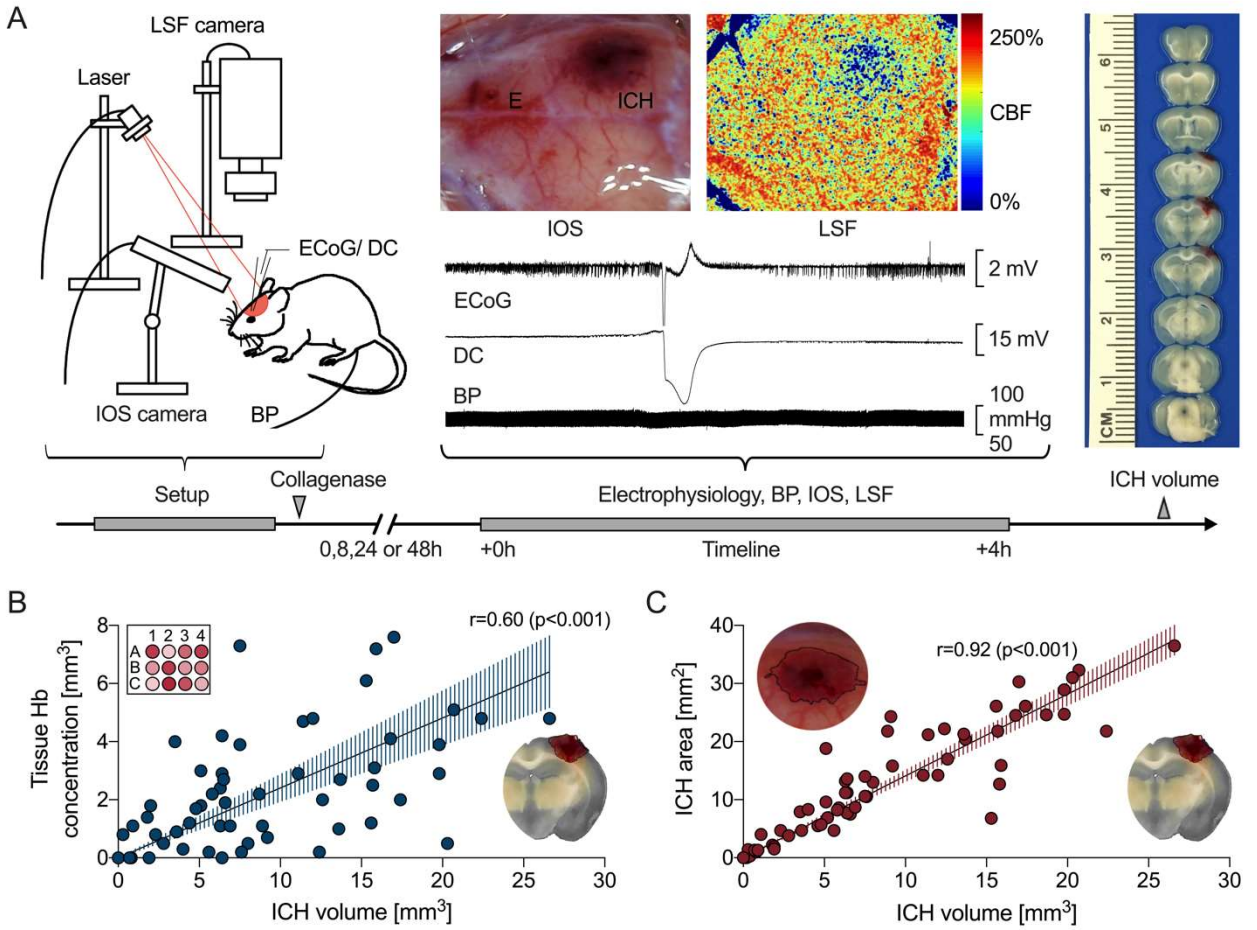

Figure 1. Experimental Design A. Experimental setup including the femoral artery catheter to monitor systemic physiology, the camera for intrinsic optical signal imaging (IOS), a second camera and near-infrared laser diode for laser speckle flowmetry (LSF), and a glass capillary microelectrode to monitor electrophysiology. The horizontal line shows the experimental timeline. Starting 0h, 8h, 24h, or 48h after collagenase injection, electrophysiology (ECoG, DC), arterial blood pressure (BP), IOS, and LSF were continuously recorded for 4h. Representative electrophysiological (DC, ECoG) and BP tracings and IOS and LSF images, obtained through the intact skull, are shown. A typical slow negative extracellular potential shift of the SD wave is seen on the DC tracing recorded by the microelectrode (E) visible on the IOS image, along with the intracerebral hemorrhage (ICH) around the collagenase injection site. LSF image shows CBF changes relative to baseline (%) as indicated in the color bar. The field of view is similar to IOS. 1-mm coronal sections were prepared at the end of the recordings to calculate ICH volume. **B.** Hemorrhage volume measured using coronal sections correlated with hemoglobin (Hb) content measured later in tissue homogenates (Spearman r=0.60, p<0.001; left panel). **C.** The dorsal area of ICH prior to sacrifice (as seen in IOS) showed a tight correlation with the ICH volume calculated post-mortem (Spearman r=0.92, p<0.001; right panel). Each dot represents a single animal.

This figure and its legend were modified from the original publication *Fischer P., Sugimoto K., Chung D.Y., Tamim I., Morais A., Takizawa T., Qin T., Gomez C. A., Schlunk F., Endres M., Yaseen M. A., Sakadzic S., Ayata C. Rapid hematoma growth triggers spreading depolarizations in experimental intracortical hemorrhage. J Cereb Blood Flow Metab. 2021;41(6):1264-76.*

point was set to 2 mm posterior and 3 mm lateral to bregma over the parietal cortex to allow for even hemorrhage propagation rostrocaudally and mediolaterally. Testing volumes of 0.2 µl and 0.4 µl (n=4), a volume of 0,2 µl of diluted collagenase VII-S was found to allow for constant injection speed using a manual injection pump while not causing backflow along the injection needle. Dilutions ranging from 0.1 - 0.8 IU/µl bacterial collagenase VII-S (n=8) were tested to induce various sizes of hemorrhage and concentrations of 0.2-0.6 IU/µl chosen for the experimental protocol yielding visible hemorrhage not exceeding the diameter of the mouse cortex (approximately 1 mm).

Based on the pilot experiments, in the final study, a 10 µl syringe connected with an injection needle (34 gauge, Small Hub RN Needle, point style 4, Hamilton Company, Reno, NV, USA) was filled with bacterial collagenase VII-S diluted in 0.9% NaCl (Sigma Aldrich, St. Louis, MO, USA) and attached to a manual injection pump. After recording baseline images for IOS- and LSF-imaging and establishing the electrophysiological recordings, the needle was then stereotactically lowered into the cortex via the posterior borehole to a depth of 0.5 mm from the cortical surface, and 0.2 µl of bacterial collagenase VII-S (0.2 – 0.6 IU/µl) were injected at a rate of 0.67 µl/min[76]. To prevent any backflow after injection, the needle was left in place for 5 min before it was carefully removed. Fresh collagenase VII-S was purchased every two to three months to prevent alterations in enzyme activity.

2.4 Imaging

IOS and LSF images were acquired simultaneously with electrophysiological recordings for 240 min after hemorrhage induction to investigate ICH growth, SD occurrence, and changes in CBF (Fig.1A).

2.4.1 Real time hematoma imaging and intrinsic optical signal

A USB camera (MU300, AmScope, Irvine, CA, USA), set up over the head of the animal, was used to image the cortical surface and track the hematoma distinctly visible through the intact skull during the 240-min recording. Images were taken every 4 sec, and hemorrhage volume and growth were calculated every 10 min, as described in detail later. The green light channel of the same images was further utilized to detect SD via charac-

teristic IOS changes, as described in detail by the group elsewhere[81]. Briefly, using software included with the USB camera, time-lapse images taken every 4 sec were saved as jpeg files and imported into MATLAB using a script. After that, difference images of two consecutive images were generated for real-time and post hoc analysis. Based on the characteristic morphology of the spreading wavefront, SDs were then detected, and the area of their origin was determined using the difference images.

2.4.2 Laser speckle flowmetry

To investigate the spatiotemporal changes of CBF during cortical hemorrhage, LSF was employed. Methodology for LSF has been extensively described previously[76, 82, 83]. Briefly, a near-infrared laser diode (785 nm) with a penetration depth of approximately 500 µm was used to illuminate the exposed skull surface diffusely, and a CCD camera (CoolSnap cf, 1392 × 1040 pixels; Photometrics, Tucson, AZ) was set up above the animal's head[76]. To compute CBF, bundles of ten consecutive raw speckle images, averaged to refine the signal-to-noise ratio, were recorded at 15 Hz and processed by using a sliding grid of 7x7 pixels to compute images of speckle contrast, a measure of speckle visibility that is associated with the velocity of scattering particles. Subsequently, speckle contrast images were transformed to images of correlation time values that express the decay time of the light intensity autocorrelation function and are linearly and inversely proportional to the mean blood velocity[84]. To monitor relative CBF changes during the experiment, the ratio of baseline correlation time values, taken prior to collagenase injection, to subsequent values was calculated every 3.5s generating laser speckle perfusion images[76] shown in Figure 1.

To analyze perihematomal CBF, a specific cortical region of interest (ROI) was defined for each animal that did develop a spontaneous SD originating from the hemorrhage at any time of the experiment or animals which did not develop any SD. In animals that did develop at least one SD, in each animal, a circular ROI (0.8 mm diameter; Fig.5A) was set over the cortical area, where the first spontaneous SD in that animal originated from. In animals that did not develop any SD, a ring ROI (0.8 mm-thick; Fig.5A) was set at the mean distance of all SD origins to the center of ICH to analyze CBF in an equivalent perimeter of ICH[76]. A total of 6 animals were excluded from CBF analysis because insufficient skull translucence prohibited precise CBF calculation using LSF.

2.5 Experimental protocols

The timeline of the basic experimental protocol of acute ICH (n=48) in which no interventions were carried out during the 4h monitoring period is displayed in Figure 1A. This protocol was modified in five subgroups of animals, as described in the following. In all subgroups, at the end of each experiment, a cotton ball soaked in 1M KCl was briefly and carefully placed on the cortex via a borehole to trigger and detect an SD confirming the integrity of the electrophysiological recording.

2.5.1 Subacute phases of cortical hemorrhage

Subacute phases of cortical hemorrhage (8-52h) were investigated in a separate cohort of n=9 animals. To reduce morbidity during the survival period, the femoral artery was not cannulated prior to hemorrhage induction in these animals. Instead, after ICH was induced by collagenase VII-S injection, the scalp was carefully sutured, and local analgesic (Lidocaine gel 2%) was applied. Mice were then returned to their home cage to recover from anesthesia. 8h, 24h, or 48h after hemorrhage induction, mice were re-anesthetized, the femoral artery catheterized, and animals imaged for 240 min as described before.

2.5.2 Normobaric hyperoxia

Normobaric hyperoxia (NBO) was induced in a subgroup of animals (n=8) after general surgical preparation and hemorrhage induction. O_2 fraction in inspiration air was increased to 100% 15 min after collagenase injection. Animals then received 100% O_2 in inspiration air for the remaining 225 min of the experiment and were imaged for the entire 240 min as described above, along with their controls that received regular inspiration gases (n=8).

2.5.3 Induced Hypertension

After regular surgical preparation and collagenase injection, at the onset of hematoma growth phase (46 ± 14 min after collagenase injection), hypertension was induced in a subgroup of animals (n=10) by an intraperitoneal injection of the α_1-adrenergic agonist phenylephrine (10 mg/kg body weight). While imaging was conducted as described above, the hypertensive effect of phenylephrine only lasted for a limited time. Therefore,

animals were sacrificed, either 30 min after phenylephrine injection, whenever no SD was triggered, or 30 min after the last observed SD, whenever SDs were triggered.

2.5.4 Focal Cerebral Ischemia

To compare the propensity of primary cortical ICH and primary focal ischemic lesions to trigger SDs, instead of cortical hemorrhage, focal cortical ischemia was induced in a subgroup of mice (n=6) by distal Middle Cerebral Artery occlusion (dMCAo) as described previously[82].

Briefly, mice were positioned in a stereotactic frame after general surgical preparation. The temporalis muscle was then dissected and removed. Next, under 0.9% NaCl-cooling, a borehole was drilled in the temporal bone overlying the distal Middle Cerebral Artery (MCA) right above the zygomatic arch. Finally, a microvascular clip was used to occlude the distal MCA while keeping the dura intact. The middle cerebral artery then remained occluded for the entire duration of the experiment while monitoring for SDs was done, equivalent to mice, in which cortical hemorrhage had been induced. After 240 min of focal cerebral ischemia, the microvascular clip was removed to check for reperfusion. Immediately after, animals were sacrificed.

2.5.5 Intracortical Glutamate and Aspartate injections

Instead of collagenase, after general surgical preparation, in a subset of animals, the excitatory amino acid glutamate was injected directly into the cortex at the identical location used for collagenase injection. Glutamate was injected with or without the excitatory amino acid aspartate. Glutamate and aspartate concentrations of fresh plasma (45µM glutamate and 5µM aspartate in 0.9% NaCl, n=6) and further increased glutamate concentrations alone (50µM glutamate in 0.9% NaCl, n=5; 100µM glutamate in 0.9% NaCl, n=5) were investigated. To mimic acute bleeding in our ICH model, we set the injection rate to the average peak ICH growth detected in animals that developed SDs in our ICH model (0,2µl/ min). We then continued injection for 20 min, the longest period we observed such an ICH growth rate. Animals were imaged for a total of 30 min, as described above. The femoral artery was not cannulated in this subgroup.

2.6 Lesion volume

2.6.1 Final hemorrhage volume

To flush intravascular blood out of the brain, mice were transcardially perfused with 30 ml of phosphate-buffered saline (PBS) under deep isoflurane anesthesia (5%) at the end of the experiment. Brains were then collected and cut into 1 mm coronal sections using an ice-cooled mouse brain matrix and razor blades. Sections were immediately photographed under standardized conditions and the hemorrhage area on each section manually outlined, measured, and integrated along the anteroposterior axis to calculate hemorrhage volume. To confirm the integrity of our measurement, later Hb content was measured in homogenized tissue samples of each animal's entirety of sections using a well-established photometric Hb assay that has been described in detail previously[85]. In short, each brain was placed in a glass tube with 3 ml of PBS, manually homogenized, and erythrocytic membranes lysed by ultrasound application for 1 min. After 30 min of centrifugation (13000 rpm, 4 °C), 250µl of supernatant was added to 1000µl of Drabkins reagent, and absorption rates determined at 540 nm using a photometer. Ultimately, Hb concentrations were calculated based on a standard curve of fresh mouse blood.

The final hemorrhage volume calculated from coronal sections correlated with the Hb content measured later in tissue homogenates (Spearman $r=0.60$, $p<0.001$; Fig.1B). Thus, only values calculated by outlining the hemorrhage on brain sections were used for the analysis.

2.6.2 Hemorrhage volume and growth during the experiment

The area of ICH overlaying the cortical surface prior to sacrifice (measured through the intact skull during the imaging period) and the ICH volume calculated post-mortem in brain sections showed a tight and linear correlation (Spearman $r=0.91$ $p<0.001$; Fig.1C). This allowed us to use the hemorrhage area visible on the cortical surface to calculate hemorrhage volume at each time of the experiment in single animals.

To do so, hemorrhage volume was measured post-mortem in each animal and divided by the superficial hemorrhage area imaged at the end of the experiment resulting in a volume/area quotient. Subsequently, the superficial hemorrhage area at any desired time of the experiment was multiplied by the calculated quotient to compute the hemorrhage volume at that time.

2.6.3 Final ischemic lesion volume

Equivalent to mice with cortical hemorrhage, animals receiving dMCAo were transcardially perfused with 30 ml of PBS under deep isoflurane anesthesia (5%) at the end of the experiment. Brains were collected and snap frozen in -40 °C cold isopentane. Using a Cryostat, brains were then cut into 20 µm sections, which were analyzed by hematoxylin and eosin staining every 1 mm[86]. Infarcts were manually outlined on each section, measured, and integrated along the anteroposterior axis to compute infarct volume. Only direct infarct volumes were calculated due to relatively small infarcts in the dMCAo model.

2.7 Rigor and statistical analysis

Whenever applicable, an investigator not involved in the study randomly assigned mice to the intervention- or control group after surgical preparation and hemorrhage induction. Blinding was not possible for IOS-image analysis, while SDs were clearly noticeable during real-time imaging. As SDs were identifiable during LSF imaging, too, CBF calculation was carried out using an automated Matlab script. Hemorrhage volume was calculated by a blinded investigator.

Data are reported in accordance with the ARRIVE guidelines and expressed as mean ± standard deviation in text or whisker (full range) and box (interquartile range) plots (horizontal line, median; +, mean) in figures. They were analyzed statistically using GraphPad/Prism 8 (GraphPad Software, San Diego, CA, USA). Data were tested for normality using the Shapiro–Wilk test. Further statistical tests, exact p-values, and sample sizes are indicated for each dataset in the text or the figure legends. $P<0.05$ was considered statistically significant. In the absence of prior experience, sample size in ICH experiments was chosen empirically to detect a 33% difference between means and a presumed standard deviation of 25% of the mean (a=0.05, b=0.10). Nine animals were excluded from the analysis due to surgical failure. One animal did not survive until subacute imaging phase.

3 Results

3.1 Spatiotemporal characteristics of spreading depolarization occurrence

3.1.1 Acute and subacute phases of cortical hemorrhage

In the acute phase of cortical hemorrhage, hematomas visibly emerged on the cortical surface approximately 20 min after collagenase VII-S injection and further expanded at a growth rate of 0.1 – 5.1 mm^3/min. Slowing down after 120-180 min, hematoma expansion usually approached a plateau at the end of the 240-min recording (Fig. 2A).

17 of the 38 mice (45%) imaged during the acute phase of cortical hemorrhage developed one or multiple SDs that were verified by the characteristic extracellular slow negative potential shift (Fig. 2A). A total of 34 SDs could be observed, which without exception, originated from the region of hemorrhage and spread throughout the entire ipsilateral hemisphere (Supplemental Movie 2).

SDs were detected 29-221 min after collagenase injection, with the majority occurring in the first 120 min of imaging, sometimes in couplets 8-19 min apart (Fig. 2C). The 20 SDs occurring in couplets were observed in earlier phases of hematoma formation, compared to 14 single SDs that occurred at later phases of acute hemorrhage (76 ± 27 vs. 120 ± 72 min after collagenase injection, respectively; p=0.04; Welch's t-test; Fig. 2C).

In contrast to the acute phase of hematoma formation, no further hematoma growth was observed at subacute stages 8-12h, 24-28h, or 48-52h after ICH induction. Likewise, not a single SD was detected in the subacute phase (n=9; p=0.01 vs. early stage; χ^2-test; Fig. 2D) despite equal hemorrhage volumes at the end of acute and subacute stages (9.6 ± 7.1 vs. 9.3 ± 5.9 mm3, respectively; n=38 and n=9; p=0.99; Mann-Whitney test; Fig. 2D).

Three sham-operated mice that received vehicle injection (0.9% NaCl) did not develop ICH during 4h of imaging (data not shown).

With no SDs occurring in subacute phases of cortical ICH in our mouse model, in subsequent experiments, we only investigated the acute phase of hematoma formation (0-4h after collagenase injection).

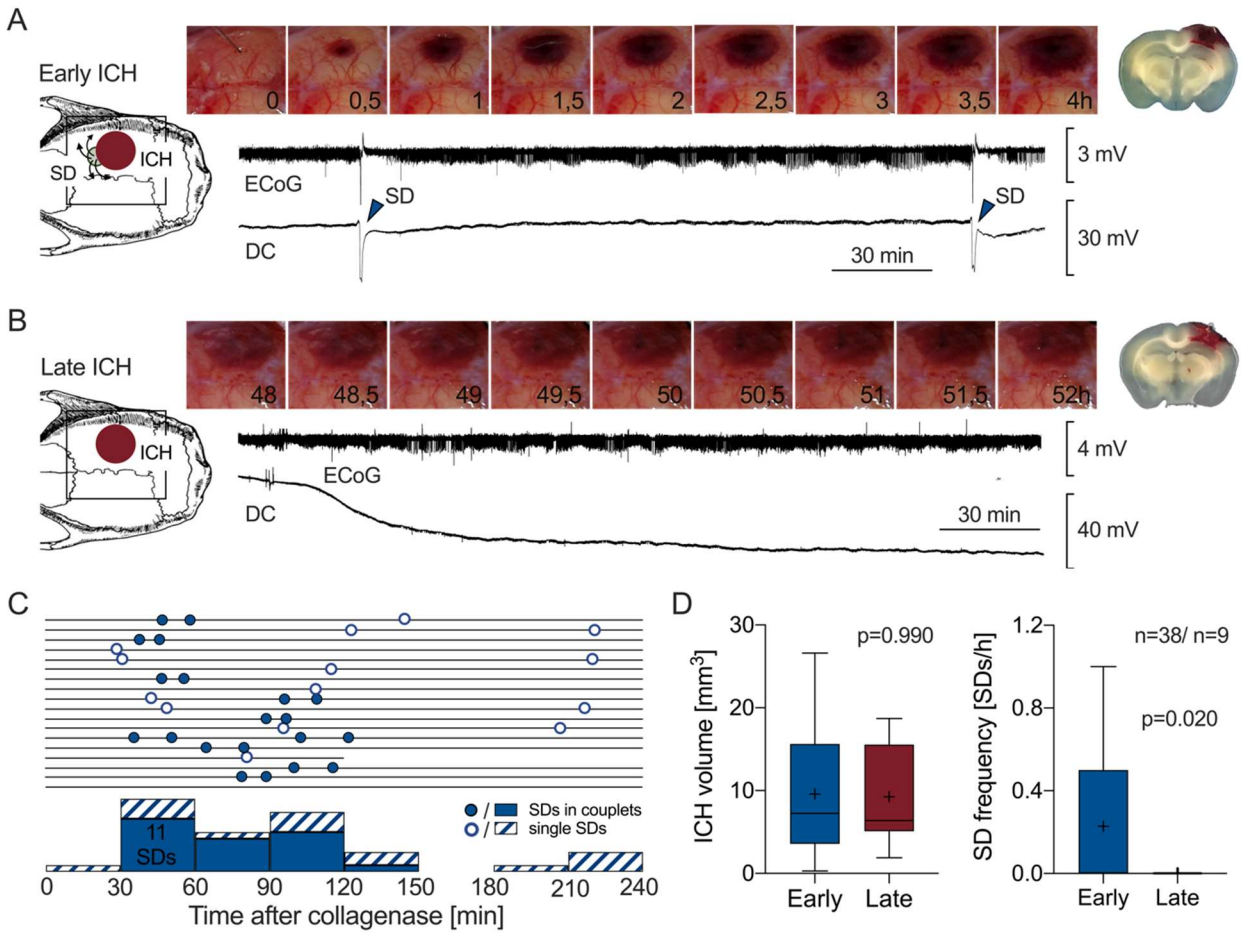

Figure 2. Spreading depolarization occurrence during acute and subacute stages of cortical hemorrhage. A. Representative intrinsic optical signal (IOS) images (every 30 min), continuous electrophysiological recordings (ECoG and DC), and a coronal brain section at the end of the experiment from an animal in the early stage of intracerebral hemorrhage (ICH) (0–4h). The left graphic shows the field of view for IOS images. The animal developed a large hematoma within 90 min. One SD emerged during this rapid growth phase, and another during a second faster growth phase later in the experiment (blue arrowheads). **B.** Representative data from an animal studied at a later stage (48–52 h) of ICH. No change in hematoma size can be seen over time. Despite the large hematoma, no SD occurred. **C.** Time of SD occurrence during the early stage of ICH in animals that developed at least one SD. Each line represents one animal. Empty circles represent single SDs, and filled circles represent SDs that occurred in couplets. Most SDs occured between 30 and 120 min after collagenase injection. SD couplets occurred in earlier phases of acute hemorrhage than single SDs. **D.** SD frequency and ICH volume is shown for early and late stages. Despite nearly identical hematoma volumes (p=0.99; Mann–Whitney test), no SD was recorded during the late stages of ICH (p=0.020 vs. early stage; Mann–Whitney test).

This figure and its legend were modified from the original publication *Fischer P., Sugimoto K., Chung D.Y., Tamim I., Morais A., Takizawa T., Qin T., Gomez C. A., Schlunk F., Endres M., Yaseen M. A., Sakadzic S., Ayata C. Rapid hematoma growth triggers spreading depolarizations in experimental intracortical hemorrhage. J Cereb Blood Flow Metab. 2021;41(6):1264-76.*

3.1.2 Acute phases of cortical hemorrhage and focal ischemic infarcts

While our data confirmed acute cortical hemorrhage to trigger SDs in the lissencephalic mouse brain, the overall SD frequency detected seemed to be lower than previously observed in focal cerebral ischemia in mice[55, 69, 87-89]. To directly compare the propensity of primary cortical ICH and primary focal ischemic lesions to trigger SDs, we Induced focal ischemic lesions in the cortices of a separate group of mice (n=6) by dMCAo and followed SD occurrence for 4h per identical protocol as in collagenase injected animals. In 5 of 6 mice developing at least one SD, a total of 26 SDs was detected (Fig. 3A), which always originated

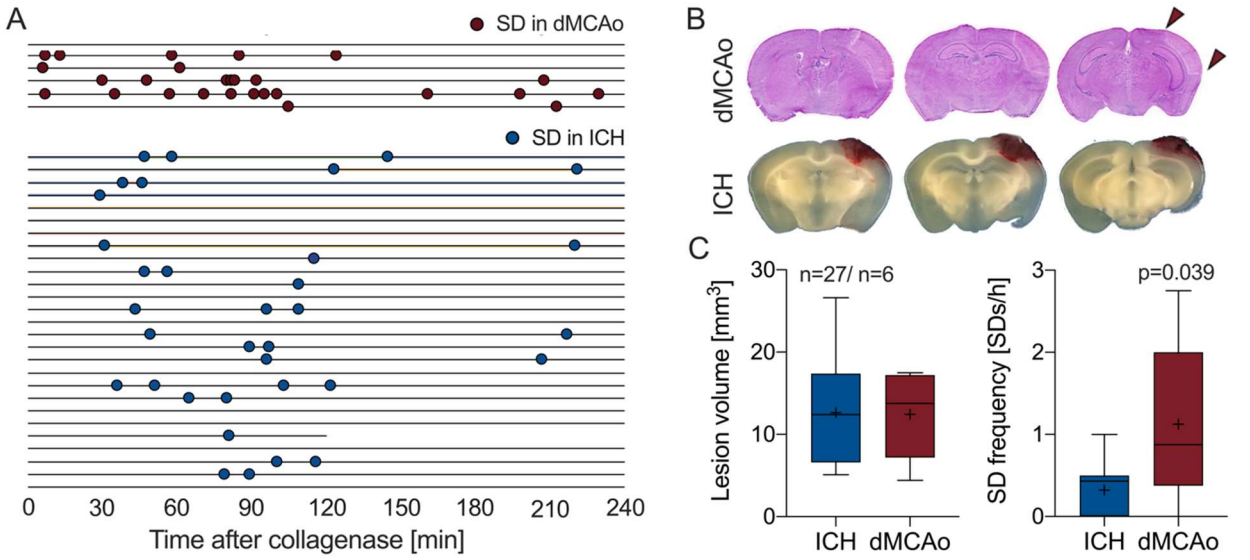

Figure 3. Propensity of primary cortical hemorrhage and primary focal ischemic infarcts to develop spreading depolarization. A. SD occurrence in primary focal ischemic infarcts caused by distal Middle Cerebral Artery occlusion (dMCAo, top) and primary hemorrhagic lesions (ICH, bottom). Each line represents one animal. Red circles represent SDs in ischemic lesions, and blue circles represent SDs that occurred in cortical hemorrhage. Five of six animals showed at least two SDs after dMCAo, while 17 of 27 animals developed at least one SD during ICH. Similar to cortical hemorrhage, most SDs in focal ischemic brains occurred during the first 2h of imaging. **B.** Representative focal ischemic lesion on H&E- stained coronal brain section 4h after dMCAo (top, red arrows) and representative cortical hemorrhage on 1-mm coronal brain section 4h after collagenase injection (bottom). Both ischemic and hemorrhagic lesions are located in nearly identical regions of the cortex. **C.** Despite identical lesion volume (left panel), ischemic lesions increased SD frequency more than threefold compared with hemorrhagic lesions (p=0.039, Mann–Whitney test; right panel). 27 of the 38 cortical hemorrhage animals with hematoma volumes matching the infarct volumes were used for this comparison.

This figure and its legend were modified from the original publication *Fischer P., Sugimoto K., Chung D.Y., Tamim I., Morais A., Takizawa T., Qin T., Gomez C. A., Schlunk F., Endres M., Yaseen M. A., Sakadzic S., Ayata C. Rapid hematoma growth triggers spreading depolarizations in experimental intracortical hemorrhage. J Cereb Blood Flow Metab. 2021;41(6):1264-76.*

from the ischemic lesion site and propagated throughout the ipsilateral hemisphere. As observed in ICH, most SDs occurred within the first 2h of the recording. However, compared with cortical hemorrhages matching in location and size (12.4 ± 5.2 vs. 12.7 ± 6.2 mm3, respectively; n=6 and n=27; p=0.94; Mann-Whitney test; Fig. 3C), ischemic lesions resulted in more than 3-fold higher SD frequencies (1.1 ± 1.0 vs. 0.3 ± 0.3 SDs/h, respectively; n=6 and n=27; p=0.04; Mann-Whitney test, Fig. 3C).

3.2 Mechanisms triggering spreading depolarization in cortical hemorrhage

3.2.1 Blood constituents and blood breakdown products

To analyze blood constituents and blood breakdown products as potential triggers for SD in cortical hemorrhage, we dichotomized mice imaged during the acute stage of ICH based on SD occurrence and first analyzed ICH volumes at the end of the 4h recording. Final hematoma volumes measured after the 240-min recording were larger in animals developing SDs than in animals not developing any SD (15.2 ± 6.1 vs. 5.0 ± 4.0 mm^3, respectively; n=17 and n=21; p<0.001; Mann-Whitney test; Fig. 4B). As reported above, however, first SDs usually occurred early in the experiment, 69 ± 32 min after hemorrhage induction, when ICH volume was still relatively small. Therefore, we plotted hematoma volume over time in animals that developed at least one SD during 240 min of recording and animals that did not (Fig. 4A and 4B) and further analyzed hematoma volume at the time when the first SD was observed in each animal. At this time of first SD occurrence, ICH volume was almost identical to the final ICH volume in animals that did not develop any SD (5.6 ± 2.8 vs. 5.0 ± 4.0 mm^3, respectively; n=17 and n=21; p=0.59; Mann-Whitney test; Fig. 4B), which argued that the amount of cortical hemorrhage itself did not correlate with SD occurrence.

While this was in line with our previous data from subacute stages of ICH where no SDs were observed despite large hemorrhage volume, to confirm our finding, we directly exposed the cortex to plasma constituents glutamate and aspartate that have been suggested to trigger SDs upon blood extravasation. Intracortical injection of 0.9% NaCl with 50µM glutamate (n=5), 100µM glutamate (n=5), or 45µM glutamate and 5µM aspartate (n=6) did not result in a single SD in any of the studied mice (data not shown).

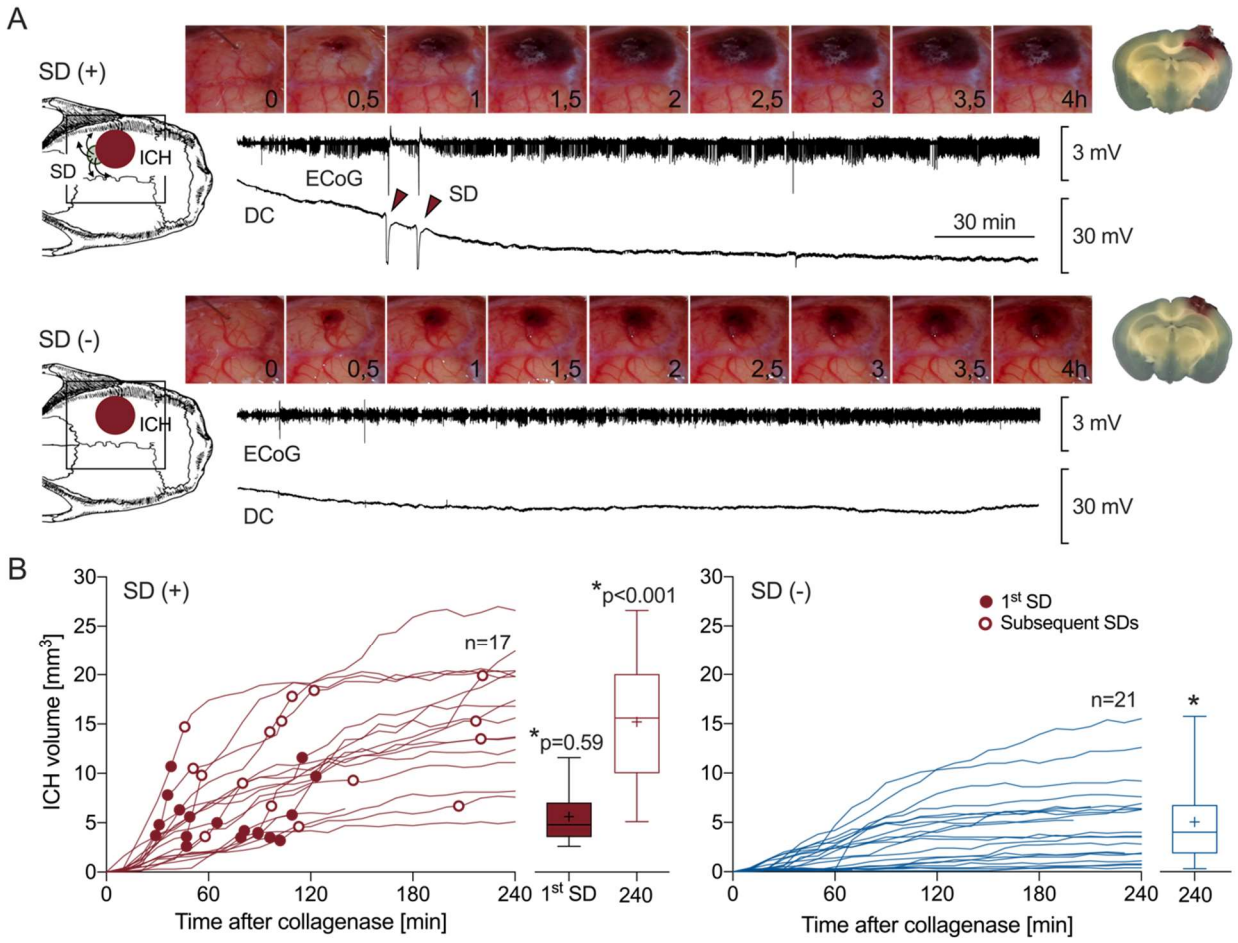

Figure 4. Hemorrhage volume and spreading depolarization occurrence. A. Representative intrinsic optical signal (IOS) images (every 30 min), continuous electrophysiological recordings (ECoG and DC), and the coronal brain section at the end of the experiment from an animal that did develop a spreading depolarization (SD (+)) and an animal that did not develop any (SD(-)) in the early stage of intracerebral hemorrhage (ICH). The left graphic shows the field of view for IOS images. In the first animal, an SD couplet occurred early in the experiment when the hematoma was still relatively small (top). The second animal did not develop any SD despite a large hematoma at the end of the experiment (bottom) **B.** ICH volume shown as a function of time in animals with SD (SD (+)) and without SD (SD(-)). Each line represents one animal. Filled circles mark the first SD. Unfilled circles mark subsequent SDs. ICH volumes at the time of first SD and the end of the experiment are shown as whisker-box plots to the right of each time course graph. ICH volumes at time of first SD (filled red whisker-box plot) were almost identical to final ICH volumes in animals that never developed an SD (empty blue whisker-box plot; p=0.59; Mann-Whitney test), while only final ICH volumes (empty red whisker-box plot) were larger in animals that did develop SDs compared to animals that did not (p<0.001; Mann-Whitney test).

This figure and its legend were modified from the original publication *Fischer P., Sugimoto K., Chung D.Y., Tamim I., Morais A., Takizawa T., Qin T., Gomez C. A., Schlunk F., Endres M., Yaseen M. A., Sakadzic S., Ayata C. Rapid hematoma growth triggers spreading depolarizations in experimental intracortical hemorrhage. J Cereb Blood Flow Metab. 2021;41(6):1264-76.*

3.2.2 Focal cortical ischemia

To test for ischemia as a possible trigger of SD in cortical ICH, we measured CBF around the hematoma by placing an ROI (0.8 mm diameter) at the point of SD origin in each mouse that developed at least one SD and compared this to CBF in an equivalent cortical region in mice that did not develop any SD (0.8 mm-thick ring ROI; Fig.5A). The CBF measured immediately before SD onset at the origin of SD (61.5 ± 16.0%) was significantly increased compared to the minimum CBF detected during the 240 min recording in both animals that developed SDs and animals that did not (41.9 ± 6.8 % and 47.6 ± 9.5 %, respectively; n=15 and n=17; $p<0.001$ and $p=0.003$; one-way ANOVA followed by Tukey's multiple comparisons; Fig. 5B), which argued against ischemia as a trigger of SD in our model. In fact, in our experiments, CBF around the hematoma never fell to levels known to trigger anoxic SDs (<30% of baseline). The lowest CBF values were usually recorded at the beginning of the experiment after the injection needle insertion, which invariably caused an SD accompanied by post-SD oligemia (Fig. 4A).

To further exclude ischemia to trigger SD, in a separate experiment, we induced NBO that is known to suppress anoxic SDs[88] and compared SD occurrence to a control group receiving regular inspiration gases (n=8 each). Elevating the oxygen fraction of inspired air to 100% O_2 15 min after hemorrhage induction increased arterial paO_2 by almost 4-fold (468 ± 36 vs. 126 ± 10 mmHg, respectively; $p<0.001$; Mann-Whitney test; data not shown), while pH, $paCO_2$, and blood pressure remained unchanged (data not shown). Nevertheless, NBO did not affect the final hematoma volume (16.2 ± 6.2 vs. 13.7 ± 5.7 mm^3, respectively; n=8 each; $p=0.51$; unpaired t-test; data not shown) and peak hemorrhage growth rate observed during the 4h monitoring period compared to controls (2.7 ± 1.4 vs. 2.4 ± 1.2 mm^3/10 min, respectively; n=8 each; $p=0.55$; Mann-Whitney test; data not shown). Likewise, the lowest CBF detected during the recording (44.0 ± 5.8 vs. 44.5 ± 7.3 % of baseline CBF, respectively; n=8 each; $p=0.88$; unpaired t-test; data not shown) and CBF immediately preceding the SD (58.3 ± 21.4 vs.56.6 ± 8.9 % of baseline CBF, respectively; n=6 and n=5, respectively; $p=0.46$; Mann-Whitney test; data not shown) did not differ in animals receiving regular inspiration gases or NBO. In line with these findings, SD frequency remained unchanged compared to controls (0.3 ± 0.3 vs. 0.3 ± 0.3 SDs/h, respectively; n=8 each; $p=0.83$; unpaired t-test; data not shown). These data further argued against ischemia triggering SDs in our hemorrhage model.

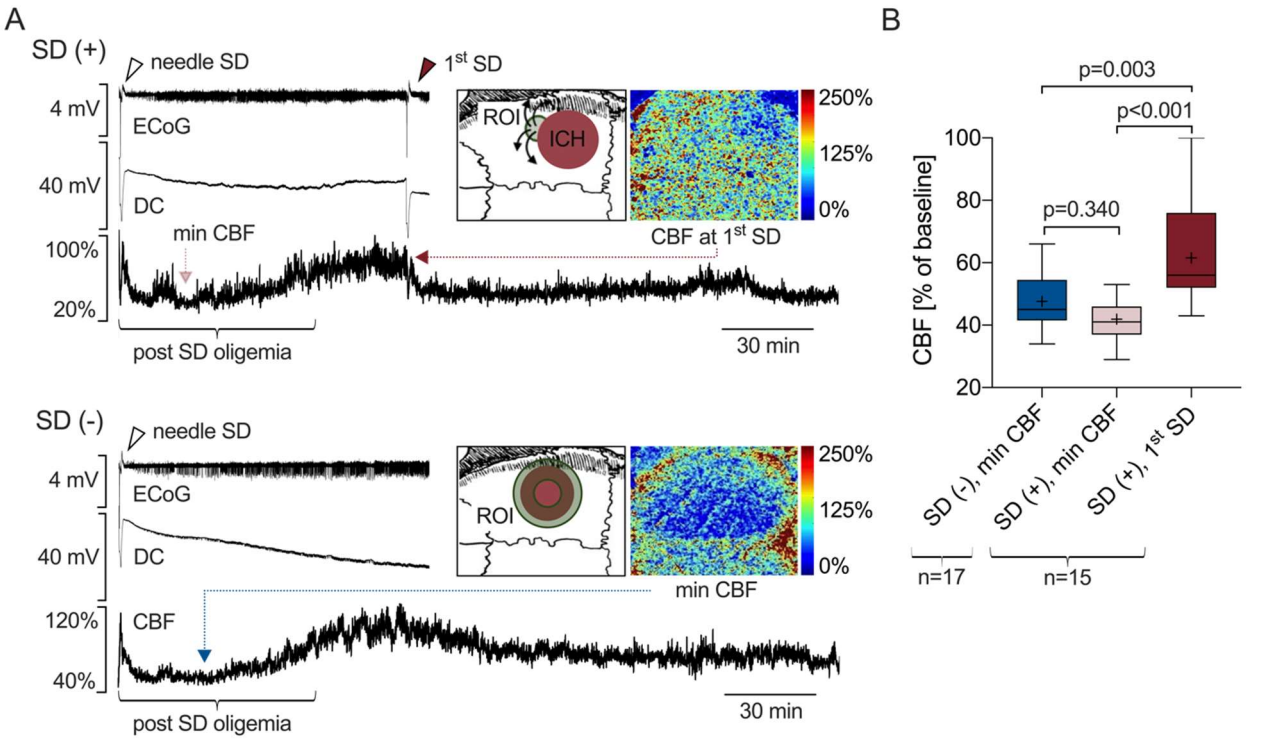

Figure 5. Cerebral blood flow and spreading depolarization occurrence. A. Representative continuous electrophysiological recordings (ECoG and DC) and continuous recording of relative cerebral blood flow (CBF) acquired through intact skull using laser speckle flowmetry (LSF) in an animal that did develop a spreading depolarization (SD (+), top) and an animal that did not develop an SD (SD(-), bottom) in the early stage of intracerebral hemorrhage (ICH). The inset shows field of view for LSF images along with the region of interest (ROI, green shaded) for CBF calculation and a representative LSF image. In animals that developed an SD, a circular ROI (0.8 mm diameter) was placed at the point of SD origin to analyze CBF changes in that ROI throughout the recording. In animals that did not develop any SD, a ring ROI (0.8 mm-thick) was placed at the average distance of all SD origins to the center of ICH to analyze CBF in an equivalent perimeter of ICH. CBF decreased to approximately 40-50% of baseline after the initial SD caused by needle insertion for collagenase injection (0 min) in both animals, typical for post-SD oligemia in mice. In the first animal, a spontaneous SD (1st SD, red arrowhead) occurred approximately 100 min after collagenase injection (top), when CBF was only mildly reduced at its origin, as seen in LSF image and CBF recording (dark red arrow). The lowest CBF was recorded during initial post-SD oligemia (min CBF, light red arrow). The second animal did not develop any SD (bottom). Again, the lowest CBF was recorded during initial post-SD oligemia, as seen in the LSF image and CBF recording (blue arrow). **B.** Minimum CBF is shown for animals that did not develop any SD during the recording. Minimum CBF as well as CBF at the onset of first spontaneous SD is shown for animals that developed an SD. Average CBF at time and place of SD origin was significantly higher than the minimum CBF levels recorded in both animals that did and animals that did not develop any SD ($p<0.001$ and $p=0.003$ vs. 1st SD; one-way ANOVA followed by Tukey's multiple comparisons test).

This figure and its legend were modified from the original publication *Fischer P., Sugimoto K., Chung D.Y., Tamim I., Morais A., Takizawa T., Qin T., Gomez C. A., Schlunk F., Endres M., Yaseen M. A., Sakadzic S., Ayata C. Rapid hematoma growth triggers spreading depolarizations in experimental intracortical hemorrhage. J Cereb Blood Flow Metab. 2021;41(6):1264-76.*

3.2.3 Hematoma growth and mechanical tissue distortion

Observing the evolving hematoma over time in the subset of animals that developed an SD, we noticed that hematoma growth usually seemed to accelerate before an SD was triggered during pronounced hemorrhage growth (Supplemental Movie 2). In contrast, no such growth dynamic seemed to exist in mice that did not develop any SD at the equivalent time of the experiment (Supplemental Movie 1), i.e., the median time when the first SD occurred after collagenase injection ($t_{1st\ SD}$ = 65 min). Therefore, we calculated ICH growth immediately preceding SDs and compared this to the growth at $t_{1st\ SD}$ in mice that did not develop any SD, as well as to the peak hemorrhage growth at any time during the 4h recording in those animals. ICH growth during the 10 min preceding an SD was twice as high as the peak growth rate (1.8 ± 1.2 vs. 0.9 ± 0.7 mm^3/10 min, respectively; n=17 and n=21; p=0.014; Mann–Whitney test; Fig.6B) and more than three times higher than the growth rate at $t_{1st\ SD}$ (1.8 ± 1.2 vs. 0.5 ± 0.7 mm^3/10 min, respectively; n=17 and n=21; p<0.001; Mann–Whitney test; Fig.6B) in animals that did not develop any SD. These data argued in favor of mechanical tissue distortion caused by the growing hematoma being associated with SD occurrence in acute cortical hemorrhage.

To further investigate mechanical tissue distortion as a potential trigger of SD in cortical hemorrhage, hypertension was pharmacologically induced in a subset of animals (n=10) to accelerate hematoma growth. Intraperitoneal phenylephrine injected at the onset of the ICH growth phase elevated baseline arterial blood pressure by 70% within 10 min (72 ± 9 vs. 122 ± 12 mmHg, respectively; n=10 each; p<0.001; paired t-test; data not shown). However, it did not significantly alter CBF around the hematoma (69.8 ± 23.7 vs. 78.9 ± 37.1 % of baseline CBF; p=0.22; paired t-test; data not shown) or systemic physiologic parameters (data not shown) compared to normotensive controls. Increased BP accelerated hematoma growth so that final hemorrhage volumes usually reached after 240 min under normotensive conditions were reached within 40 min after phenylephrine injection (9.6 ± 7.1 vs. 8.8 ± 5.2 mm^3, respectively; n=38 and n=10; p=0.915; Mann–Whitney test; data not shown). Peak ICH growth rate was increased nearly threefold in hypertensive animals compared with normotensive controls (4.6 ± 3.1 vs. 1.7 ± 1.3 mm^3/10 min; p=0.003, Mann–Whitney test; data not shown), SD frequency even 4 times higher (0.8 ± 1.2 vs. 0.2 ± 0.3 SDs/h, respectively; p=0.05; Mann–Whitney test; data not shown).

In contrast to this severe increase in overall SD frequency, however, only 60% of hypertensive animals developed SDs, which was not significantly higher than in the

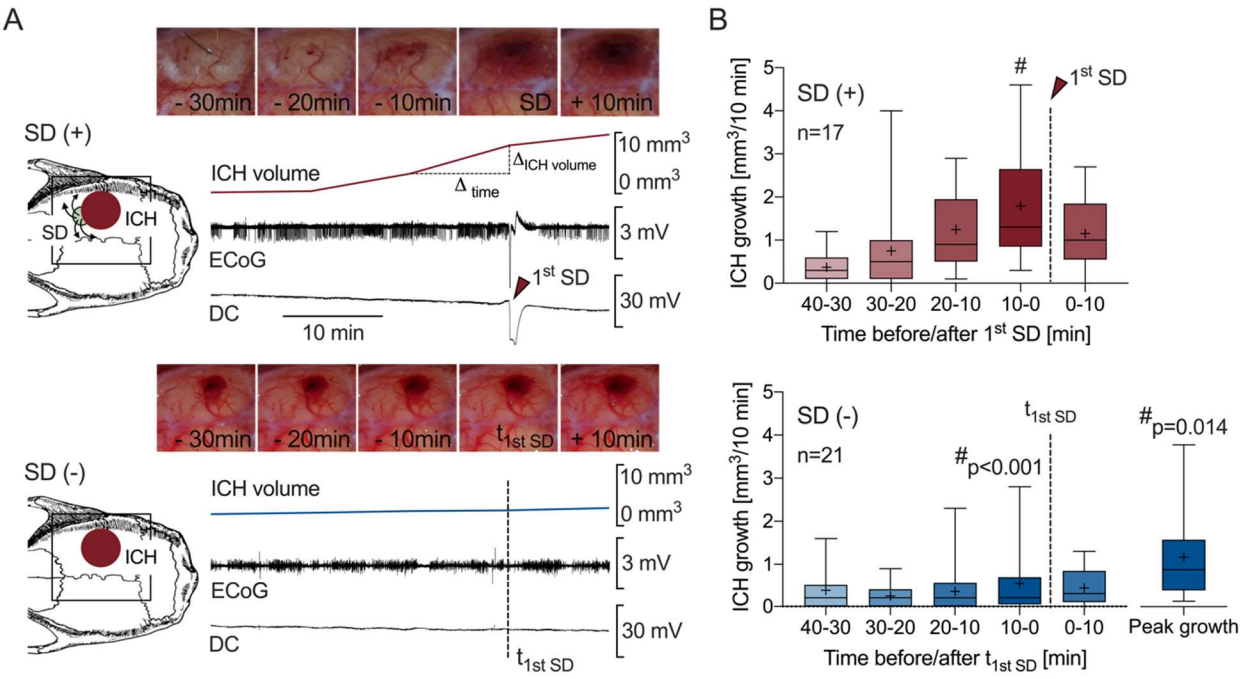

Figure 6. Hemorrhage growth rate and spreading depolarization occurrence. A. Representative intrinsic optical signal (IOS) images (every 10 min) with corresponding calculated hemorrhage volume (ICH volume), as well as continuous electrophysiological recordings (ECoG and DC) shown before and after the 1st SD in animals that developed one (SD (+), top), and the average of first SD time points ($t_{1st\ SD}$) in animals that did not develop any SD (SD (-), bottom). Left graphic shows the field of view for IOS images. In the first animal, hematoma growth (slope of the volume curve, calculated by $\Delta_{ICH\ volume} / \Delta_{time}$) accelerated severely after initial slow growth until a SD was triggered at peak growth rate. At an equivalent time of the experiment in the second animal, hematoma growth was slow throughout the recording and no SD was triggered (bottom) **B.** ICH growth per 10-min intervals is shown before and after the first SD (top) or $t_{1st\ SD}$ (bottom). ICH growth increased and peaked right before an SD (top), while no such dynamic was observed in animals not developing any SD (bottom). ICH growth during the 10 minutes immediately preceding the first SD was significantly higher than growth at an equivalent time point, as well as the peak growth at any time, in animals that did not develop an SD ($p<0.001$ or $p=0.014$, respectively, Mann–Whitney test).

This figure and its legend were modified from the original publication *Fischer P., Sugimoto K., Chung D.Y., Tamim I., Morais A., Takizawa T., Qin T., Gomez C. A., Schlunk F., Endres M., Yaseen M. A., Sakadzic S., Ayata C. Rapid hematoma growth triggers spreading depolarizations in experimental intracortical hemorrhage. J Cereb Blood Flow Metab. 2021;41(6):1264-76.*

normotensive controls (45%; p=0.390; χ^2-test; data not shown). Dichotomizing the hypertensive animals based on SD occurrence, we found ICH growth rates immediately preceding an SD to be more than three times higher than peak growth rates in animals that did not develop an SD (6.5 ± 2.3 vs. 1.8 ± 1.1 mm^3/10 min, respectively; n=6 and n=4;

p=0.003; Welch's t-test; data not shown) indicating that under hypertensive conditions, fast hematoma growth was requisite for SD occurrence, too. Or in other words, that SD was only triggered when hypertension successfully accelerated hematoma growth.

Finally, using a multiple linear regression model to analyze the entire cohort of animals monitored in the acute phase of hemorrhage (independent variables: peak ICH growth rate, final ICH volume, lowest CBF; dependent variable: SD frequency; n=48), we found SD frequency to be correlated with peak ICH growth rate (β=0.100, p=0.046) but not the final ICH volume (β=0.014, p=0.35) or lowest CBF reached during the 240-min recording (β=-0.002, p=0.89).

4 Discussion

4.1 Conclusion

In the presented study, we modified the existing mouse model of striatal ICH, induced by collagenase VII-S injection, to create a strictly cortical ICH. Our tailor-made cortical hemorrhage model allowed for a multimodal minimally invasive monitoring approach using electrophysiological tools, LSF-, and IOS imaging which enabled us to simultaneously monitor hemorrhage growth and cerebral blood flow along with SD occurrence.

We present a comprehensive investigation of SD's natural history and show SDs originating from the hematoma to occur in almost half of mice during acute stages of ICH (0-4h). SD frequencies observed in ICH are found to be three-fold lower than those observed in cortical ischemic infarcts.

Shedding new light on the mechanisms triggering SD in ICH, we show that SD does not appear in subacute stages of ICH (8-52h). Comparing animals that do and animals that do not develop spontaneous SDs, we prove SD occurrence to not depend on hematoma size or perihematomal perfusion. Moreover, we show that plasma concentrations of glutamate and aspartate directly injected into the cortex do not trigger SDs. Likewise, we demonstrate that normobaric hyperoxia does not affect SD frequency.

Instead, we observe SDs to occur during phases of rapid hematoma growth. In a separate cohort, we accelerate hematoma growth via induced hypertension and yield a four-fold increase in SD frequency. Ultimately, we show SD occurrence to be correlated with peak ICH growth but not final ICH volume or lowest CBF recorded using a multiple linear regression analysis of the entity of animals monitored in the acute phase of ICH.

4.2 Spatiotemporal characteristics of spreading depolarization occurrence

Our data provide evidence that spontaneous SDs occur in a mouse model of acute but not subacute cortical ICH. Using a minimally invasive monitoring approach, we show that temporal characteristics of SD occurrence in acute cortical ICH in the mouse closely match those reported in two relatively small cohorts of acute ICH induced by collagenase injection in the gyrencephalic swine[35, 36]. Here SDs occur as early as 17 or 38 min after

hemorrhage induction and decrease in frequency within the first hours of the recording[36]. Demonstrating SD to originate from the hematoma boundaries, which has likewise been reported in swine[35-37], we confirm SD to be a species-independent phenomenon in acute ICH that follows similar spatial and temporal characteristics in large animals gyrencephalic brain and the lissencephalic mouse brain.

To contextualize the findings from our ICH model, we compare them with another brain injury, ischemic stroke, in which temporal and spatial characteristics of SD occurrence have been extensively studied in murine models[55, 69, 87]. To do so, we use a standardized model under identical experimental conditions for both ischemic and hemorrhagic stroke. We investigate the propensity of focal ischemia and primary cortical hemorrhage matched for size and location to trigger SDs and find focal ischemic lesions to be a more potent trigger for SD than primary ICH. Recorded SD frequencies in our focal ischemic model go in line with previous studies reporting similar SD frequencies in experimental focal ischemia[55, 69]. Finally, we prove that SD frequency in primary ICH drastically increases under hypertensive conditions, the most common primary pathoetiology of clinical ICH[12]. Here, SD frequencies similar to those seen in focal ischemic brains[55, 69] are observed.

In stark contrast to acute stages, we do not detect a single SD at subacute stages of ICH (8-52h after hemorrhage onset), albeit two studies of experimental ICH in the swine have shown SD to occur multiple hours after hemorrhage induction[35, 37]. Lacking data on time course of hematoma formation and possible SD triggers in the existing studies of porcine ICH prohibit in depth analysis of the conflicting results of the presented data and porcine studies. However, some differences in the used experimental protocols can be carefully considered. First, in the porcine study that used the collagenase model, heparin was added to injected collagenase[35], while in our study collagenase was solely dissolved in NaCl. This cortical injection of heparin might have prolonged the phase of hematoma formation. Second, in the same study, even in porcine control cohorts only injected with saline or no substance at all, SDs were observed in the absence of ICH for multiple hours after needle insertion, suggesting a mechanism triggering SD that was not necessarily related to ICH[35]. In our experimental setup, sham controls injected with saline did not develop a single SD. Last, the recording of SD in both experimental swine studies required subdural electrode placement established via a craniotomy[35-37], resulting in an experimental setup that was more invasive than our cautious experimental approach and might have influenced SD occurrence.

4.3 Mechanisms triggering spreading depolarization in cortical hemorrhage

4.3.1 Blood constituents and blood breakdown products

To date, neither blood constituents nor blood breakdown products have been investigated as potential SD triggers in experimental ICH. As blood inarguably extravasates during ICH, we hypothesized blood constituents like glutamate or breakdown products like K^+ and Hb to trigger SD in our model of cortical ICH. Yet, our data strongly argue against SD occurrence in cortical ICH being related to blood constituents or breakdown products.

First, we investigate blood constituents as potential SD triggers. Following hematoma expansion during the 240-min recording, we note that the hemorrhage volume immediately preceding an SD is not larger than the final hemorrhage volume in animals not developing any SD and therefore does not predict SD occurrence. A multiple linear regression analysis of all animals imaged during acute ICH (0-4h) confirms this finding. It shows that final hemorrhage volume does not correlate with SD frequency, which would have been expected if blood constituents triggered SD. Our data are in line with a recent study that showed fresh blood applied onto the pial surface to not trigger SD in rodents[56] and another previous study investigating porcine cortical ICH, in which autologous arterial blood injection into the right frontal lobe resulted in SDs in only one of eight animals monitored during the first 4h of the recording[37]. However, we aim to strengthen our finding by injecting plasma concentrations of glutamate or even higher concentrations with and without aspartate directly into the cortex. Showing that these, even when injected at rates closely mimicking peak hemorrhage growth, do not trigger SD either, we exclude the excitatory amino acid glutamate as a trigger for SD in our ICH model and confirm previous studies that have shown topical application of up to 20000 µM glutamate[90, 91] or intracortical iontophoresis using 500000 µM glutamate[92] to not trigger SD.

Second, we analyze blood breakdown products as possible SD triggers in ICH. Whether blood breakdown products can cause SD has been investigated for over four decades[59, 60, 93] but remains controversial, especially in the context of SAH[56-58]. Despite large hematomas in animals imaged in subacute stages, in our experiments, not a single SD is observed later than 4h after hemorrhage onset when hemorrhage growth has reached a plateau. If blood breakdown products triggered SD in ICH, they should have done so mainly in subacute stages of our model, when arguably hemolysis, which develops over

hours to days, is present[11, 94-98]. Notably, this absence of SD in subacute stages of cerebral hemorrhage has also been observed in a mouse model of SAH[56]. Here pial application of fresh blood without prior in vitro hemolysis did not trigger a single SD in a cohort of mice observed for 72h[56] while, in stark contrast to this, blood hemolyzed prior to application did trigger SD[56]. This is particularly of interest as it was shown more than 20 years ago that in the subarachnoid space, synergistic effects of K^+ and Hb can cause spreading ischemia in the rat when applied in concentrations of in vitro hemolyzed blood[59, 60]. In this context, Hb acts as a NO scavenger reducing NO availability, which results in a pronounced reduction of the K^+ threshold to trigger SD[57, 61]. While K^+ and Hb concentrations in ex vivo hemolyzed blood trigger SD[56, 59, 60], our data thus add to the evidence that blood breakdown product concentrations do not reach levels high enough to trigger SD during in vivo hemolysis, at least in the lissencephalic mouse brain. Importantly, if blood breakdown products of in vivo hemolysis triggered SD, they should have done so especially in our ICH model because ICH provides an enclosed room where breakdown products like K^+ and Hb could accumulate. In contrast, murine SAH models provide no such room so that the injected blood and its breakdown products likely dissipate quickly.

Limiting the precision of our purely intracortical ICH model, in some cases, hematomas seemed to leak into the subarachnoid space, allegedly along the track of the removed needle used for collagenase application. Yet, this subarachnoid leakage was more frequently observed at later stages of acute hemorrhage, where only few SDs occurred, and most common in subacute stages, where no SDs were observed. Therefore, subarachnoid blood likely did not trigger the observed SDs, although we did not directly measure it.

4.3.2 Focal cortical ischemia

SDs occur in nearly all ischemic strokes, both clinically[40, 43, 48, 62] and experimentally[55, 69, 87]. They are triggered when transiently reduced supply (i.e., ischemia or hypoxia) or increased demand worsen supply-demand mismatch in the ischemic penumbra[55]. In SAH, intracranial pressure spikes[43] and the mass effect of blood clots[57] have been suggested to worsen supply-demand-mismatch by altering tissue perfusion and thereby triggering SDs. We hypothesized vessel rupture[12] or perihematomal tissue distortion[99] to yield ischemic conditions in ICH sufficient to trigger SD.

Using various experimental approaches, we collect convincing evidence that focal cortical ischemia or increased metabolic demand resulting in worsened supply-demand mismatch do not trigger SDs in our ICH model. First, we use high-resolution laser speckle flowmetry to show that CBF never drops to levels known to trigger anoxic depolarization (< 30 % of baseline CBF). We then prove CBF immediately preceding SD occurrence to be significantly and about a third higher than the lowest CBF recorded in both animals that do and animals that do not develop any SD. If regional hypoperfusion resulting in ischemia or hypoxia would have caused the observed SDs, the opposite, reduced CBF at SD occurrence, would have been expected. Using an ROI with a diameter of 0.8 mm for CBF measurements, we clearly should have detected any regional hypoperfusion large enough to trigger SD as the minimum tissue amount of depolarization needed to trigger an SD in the murine brain is thought to be approximately 1 mm^3 [54]. Importantly, we do not observe any interference between LSF signal and blood overlaying the cortical surface unless the blood forms a thick clot. Having that said, a decrease of LSF signal by blood would cause artificially low CBF values and would therefore not confound our conclusion.

In a different experimental approach, we show NBO, known to decrease SD frequency exclusively in focal ischemic brains by up to 60%[88], not to influence SD occurrence in cortical ICH. Because we do not measure tissue oxygenation or intracranial pressure directly and as LSF may miss tissue perfusion microheterogeneity within the ROI, we use this second approach to strengthen our finding and exclude relevant supply-demand-mismatch that could have triggered SD. Moreover, we prove induced hypertension to distinctly increase SD frequency without altering CBF compared to normotensive controls. Again, this argues against ischemia or hypoxia triggering SD in our ICH model, as induced hypertension has been shown not to affect SD occurrence in focal ischemia[100].

4.3.3 Mechanical tissue distortion

Mechanical stimulation is a well-known trigger for SD and the mass effect of the expanding hematoma is an elementary primary injury mechanism in ICH[14, 15]. It can cause local physical disruption of tissue, more widespread mechanical injury due to midline shift and herniation[15], and even shear local arterioles causing secondary hemorrhage[101]. In our study, we hypothesized mechanical tissue distortion caused by the mass effect of the growing hematoma to trigger SD.

While we do not measure peri-hematomal pressure directly because this would be invasive and might affect SD occurrence, overall, we provide various indirect evidence for mechanical tissue distortion to trigger SD in our ICH model using rapid hematoma growth as a surrogate parameter. First, we observe SDs in acute stages of ICH to emerge from the vicinity of the hematoma during phases of rapid growth, while no SDs are detected in later phases where hematoma volume has already reached a plateau and does not grow further. Second, we prove hemorrhage growth to accelerate and peak right before an SD is triggered. Finally, we show hemorrhage growth immediately preceding an SD to be twice as high as maximal growth values recorded in animals not developing any SD.

In a separate cohort, we then pharmacologically increase BP by a phenylephrine injection to account for hypertension as the most common pathoetiology of clinical ICH[10, 12]. We show induced hypertension to accelerate hemorrhage growth and increase SD frequency distinctly despite equally large hematomas in normotensive controls. Further confirming our data, equivalent to normotensive animals, again SD is only triggered in hypertensive animals that show severe hemorrhage growth prior to SD occurrence. We finally show that SD occurrence correlates with peak ICH growth but not final ICH volume or lowest CBF recorded in a multiple linear regression model of normotensive and hypertensive animals investigated during acute ICH.

Aware of our indirect approach that uses hemorrhage growth as a surrogate parameter, we justify the conclusion of mechanical pressure triggering SD by convincingly excluding other possible SD triggers that could result from rapid hematoma growth, namely ischemia, blood constituents, or breakdown products. In the conceptional design of our study, we decided the benefits of our minimally invasive multimodal imaging approach to outweigh missing direct measurements of perihematomal pressure or any blood constituents. Of course, this limits the implications of our study as we cannot exclude that a yet unidentified blood constituent caused SDs in our ICH model. This unknown constituent could be present only during rapid hematoma growth and dissipate quickly to directly trigger SDs in our ICH model or at least act synergistically with mechanical tissue distortion to trigger SD, as recently discussed for various triggers in the context of SAH[57]. However, as mentioned before, even direct injection of 3ml of autologous arterial blood into the right frontal lobe in swine only resulted in SDs in one of eight animals within the first 4h after blood injection[37], which argues against such an unknown trigger.

Finally, we could not predict where and when an SD was triggered in our model. Therefore, it would have been nearly impossible to conduct measurements at the exact point of SD occurrence, even if we decided to leave our minimally invasive monitoring approach using micro-dialysis, for example. Importantly, the injected collagenase VII-S itself does not trigger SD, as SDs occur with a latency of more than 25 minutes, and not a single SD is triggered during collagenase VII-S injection.

4.4 Implications for clinical translation

In humans, SD has predominantly been investigated in subacute deep lobar and basal ganglia ICH cases. Here, various studies have shown SDs to occur in about two-thirds of patients with large ICH and to peak 1-2 days after ictus[40, 42, 44-46]. Despite evidence of SD in subacute clinical ICH[40, 42, 44-46], we do not detect any SDs in subacute stages (8-52h) of cortical ICH in our mouse model, as discussed above. Therefore, it could be speculated that in subacute stages of human ICH, mechanisms trigger SD that do not exist in our cortical ICH model or at least do not contribute relevantly. Interestingly, in both a study of 27 patients[42] and a case report[44], an association of SD occurrence with perihematomal edema progression was observed, which might have been absent in our model due to relatively small purely cortical hematomas. Perihematomal edema typically evolves relatively slowly, hours to days after hemorrhage onset[102-104], and therefore should have been peaking in subacute, not acute, stages of our ICH model where SDs typically occurred. These conflicting findings might limit translational implications of our data for subacute clinical ICH. However, the external validity of existing clinical findings must be considered carefully for cases of spontaneous ICH without any intervention, too. This is because, in all the investigated patients to date, craniotomy or craniectomy had previously been performed for hematoma evacuation while only in the event of surgery by medical indication subdural electrode strips were placed to record electrocorticography[40, 42, 44-46]. These invasive interventions might have influenced SD occurrence and stand in contrast to our mouse model, in which we aimed for a minimally invasive monitoring approach.

Unlike in subacute ICH, SD has not been investigated in acute ICH in a clinical setting because craniotomy or craniectomy for hematoma evacuation was needed to place intracranial recording electrodes in the existing clinical studies and therefore prohibited monitoring during acute ICH[40, 42, 44-46]. Thus, we do not know whether SD occurs in acute ICH

in humans, although SD occurrence during acute porcine cortical ICH is well documented in the experimental setting[35-37]. In this context, one might argue that the experimental collagenase model, which is thought to disrupt multiple vessel types, including the capillary bed[14, 25, 78-80, 105, 106], might not precisely represent clinical ICH which is usually caused by the rupture of a single arteriole initially. Yet, in our ICH model, hematoma growth often shows sudden surges superimposed on a steady but slower pace of expansion, which likely is triggered by arterial rupture rather than capillary oozing. Finally, the source of the bleeding does not affect our conclusions. In summary, it therefore does not seem far-fetched that the mass effect of a growing hemorrhage, large enough to trigger midline shift, could trigger mechanical SDs in the human brain, too.

Interestingly, in patients suffering from CAA, a common primary etiology of ICH, transient focal neurologic episodes can be observed that often show clinical features similar to migraine aura[107, 108]. These typically short and completely reversible focal sensory or motor symptoms often show a spreading pattern propagating to adjacent body parts congruent with cortical somatotopy[107, 108], which is considered almost pathognomonic for SD[13]. As such, the frequently observed transient focal neurologic episodes in CAA might at least partially indicate SD caused by the mass effect of growing microbleeds.

4.5 Future perspectives

In conclusion, our data suggest SD is a neurophysiological phenomenon in ICH that follows similar temporal and spatial characteristics throughout different species. It implicates mechanical tissue distortion to trigger SD in murine cortical ICH, with other hypothesized triggers like blood constituents and breakdown products or focal ischemia not contributing to a significant extent.

Only further clinical research will prove whether mechanical pressure can trigger SD in patients suffering from acute ICH, too. In fact, a novel monitoring approach has recently been used to monitor SDs through the intact skull in humans[109] and might allow for early noninvasive SD monitoring in patients with acute ICH in the near future. In addition, experimental studies might show whether SD is just an epiphenomenon or plays a role in the complex pathophysiology of ICH.

5 References

1. Feigin VL, Lawes CM, Bennett DA, Anderson CS. Stroke epidemiology: A review of population-based studies of incidence, prevalence, and case-fatality in the late 20th century. *Lancet Neurol*. 2003;2:43-53
2. Greenberg SM, Ziai WC, Cordonnier C, Dowlatshahi D, Francis B, Goldstein JN, Hemphill JC, 3rd, Johnson R, Keigher KM, Mack WJ, Mocco J, Newton EJ, Ruff IM, Sansing LH, Schulman S, Selim MH, Sheth KN, Sprigg N, Sunnerhagen KS, American Heart Association/American Stroke A. 2022 guideline for the management of patients with spontaneous intracerebral hemorrhage: A guideline from the american heart association/american stroke association. *Stroke*. 2022;53:e282-e361
3. Krishnamurthi RV, Ikeda T, Feigin VL. Global, regional and country-specific burden of ischaemic stroke, intracerebral haemorrhage and subarachnoid haemorrhage: A systematic analysis of the global burden of disease study 2017. *Neuroepidemiology*. 2020;54:171-179
4. Zille M, Farr TD, Keep RF, Romer C, Xi G, Boltze J. Novel targets, treatments, and advanced models for intracerebral haemorrhage. *EBioMedicine*. 2022;76:103880
5. Jolink WM, Klijn CJ, Brouwers PJ, Kappelle LJ, Vaartjes I. Time trends in incidence, case fatality, and mortality of intracerebral hemorrhage. *Neurology*. 2015;85:1318-1324
6. van Asch CJ, Luitse MJ, Rinkel GJ, van der Tweel I, Algra A, Klijn CJ. Incidence, case fatality, and functional outcome of intracerebral haemorrhage over time, according to age, sex, and ethnic origin: A systematic review and meta-analysis. *Lancet Neurol*. 2010;9:167-176
7. Poon MT, Fonville AF, Al-Shahi Salman R. Long-term prognosis after intracerebral haemorrhage: Systematic review and meta-analysis. *J Neurol Neurosurg Psychiatry*. 2014;85:660-667
8. Flaherty ML, Haverbusch M, Sekar P, Kissela B, Kleindorfer D, Moomaw CJ, Sauerbeck L, Schneider A, Broderick JP, Woo D. Long-term mortality after intracerebral hemorrhage. *Neurology*. 2006;66:1182-1186
9. An SJ, Kim TJ, Yoon BW. Epidemiology, risk factors, and clinical features of intracerebral hemorrhage: An update. *J Stroke*. 2017;19:3-10

10. Sadaf H, Desai VR, Misra V, Golanov E, Hegde ML, Villapol S, Karmonik C, Regnier-Golanov A, Sayenko D, Horner PJ, Krencik R, Weng YL, Vahidy FS, Britz GW. A contemporary review of therapeutic and regenerative management of intracerebral hemorrhage. *Ann Clin Transl Neurol*. 2021;8:2211-2221
11. Xi G, Keep RF, Hoff JT. Mechanisms of brain injury after intracerebral haemorrhage. *Lancet Neurol*. 2006;5:53-63
12. Keep RF, Hua Y, Xi G. Intracerebral haemorrhage: Mechanisms of injury and therapeutic targets. *Lancet Neurol*. 2012;11:720-731
13. Smith EE, Charidimou A, Ayata C, Werring DJ, Greenberg SM. Cerebral amyloid angiopathy-related transient focal neurologic episodes. *Neurology*. 2021;97:231-238
14. Schlunk F, Greenberg SM. The pathophysiology of intracerebral hemorrhage formation and expansion. *Transl Stroke Res*. 2015;6:257-263
15. Magid-Bernstein J, Girard R, Polster S, Srinath A, Romanos S, Awad IA, Sansing LH. Cerebral hemorrhage: Pathophysiology, treatment, and future directions. *Circ Res*. 2022;130:1204-1229
16. Flaherty ML. Anticoagulant-associated intracerebral hemorrhage. *Semin Neurol*. 2010;30:565-572
17. Poon MT, Bell SM, Al-Shahi Salman R. Epidemiology of intracerebral haemorrhage. *Front Neurol Neurosci*. 2015;37:1-12
18. Herweh C, Juttler E, Schellinger PD, Klotz E, Jenetzky E, Orakcioglu B, Sartor K, Schramm P. Evidence against a perihemorrhagic penumbra provided by perfusion computed tomography. *Stroke*. 2007;38:2941-2947
19. Orakcioglu B, Fiebach JB, Steiner T, Kollmar R, Juttler E, Becker K, Schwab S, Heiland S, Meyding-Lamade UK, Schellinger PD. Evolution of early perihemorrhagic changes--ischemia vs. Edema: An mri study in rats. *Exp Neurol*. 2005;193:369-376
20. Schellinger PD, Fiebach JB, Hoffmann K, Becker K, Orakcioglu B, Kollmar R, Juttler E, Schramm P, Schwab S, Sartor K, Hacke W. Stroke mri in intracerebral hemorrhage: Is there a perihemorrhagic penumbra? *Stroke*. 2003;34:1674-1679
21. Qureshi AI, Wilson DA, Hanley DF, Traystman RJ. No evidence for an ischemic penumbra in massive experimental intracerebral hemorrhage. *Neurology*. 1999;52:266-272

22. Zazulia AR, Diringer MN, Videen TO, Adams RE, Yundt K, Aiyagari V, Grubb RL, Jr., Powers WJ. Hypoperfusion without ischemia surrounding acute intracerebral hemorrhage. *J Cereb Blood Flow Metab*. 2001;21:804-810
23. Mayer SA, Lignelli A, Fink ME, Kessler DB, Thomas CE, Swarup R, Van Heertum RL. Perilesional blood flow and edema formation in acute intracerebral hemorrhage: A spect study. *Stroke*. 1998;29:1791-1798
24. Murakami M, Fujioka S, Oyama T, Kuroda J, Tajiri S, Kuratsu J. Serial changes in the regional cerebral blood flow of patients with hypertensive intracerebral hemorrhage -- long-term follow-up spect study. *J Neurosurg Sci*. 2005;49:117-124
25. Kirkman MA, Allan SM, Parry-Jones AR. Experimental intracerebral hemorrhage: Avoiding pitfalls in translational research. *J Cereb Blood Flow Metab*. 2011;31:2135-2151
26. Wilkinson DA, Pandey AS, Thompson BG, Keep RF, Hua Y, Xi G. Injury mechanisms in acute intracerebral hemorrhage. *Neuropharmacology*. 2018;134:240-248
27. Somjen GG. Mechanisms of spreading depression and hypoxic spreading depression-like depolarization. *Physiol Rev*. 2001;81:1065-1096
28. Dreier JP. The role of spreading depression, spreading depolarization and spreading ischemia in neurological disease. *Nat Med*. 2011;17:439-447
29. Dreier JP, Reiffurth C. The stroke-migraine depolarization continuum. *Neuron*. 2015;86:902-922
30. Leao A. Spreading depression of activity in the cerebral cortex. *Journal of Neurophysiology*. 1944;7:359-390
31. Rounds HD. Kc1-induced 'spreading depression' in the cockroach. *J Insect Physiol*. 1967;13:869-872
32. Terai H, Gwedela MNV, Kawakami K, Aizawa H. Electrophysiological and pharmacological characterization of spreading depolarization in the adult zebrafish tectum. *J Neurophysiol*. 2021;126:1934-1942
33. Lauritzen M, Rice ME, Okada Y, Nicholson C. Quisqualate, kainate and nmda can initiate spreading depression in the turtle cerebellum. *Brain Res*. 1988;475:317-327
34. Ayata C, Lauritzen M. Spreading depression, spreading depolarizations, and the cerebral vasculature. *Physiol Rev*. 2015;95:953-993

35. Mun-Bryce S, Roberts L, Bartolo A, Okada Y. Transhemispheric depolarizations persist in the intracerebral hemorrhage swine brain following corpus callosal transection. *Brain Res*. 2006;1073-1074:481-490
36. Mun-Bryce S, Wilkerson AC, Papuashvili N, Okada YC. Recurring episodes of spreading depression are spontaneously elicited by an intracerebral hemorrhage in the swine. *Brain Res*. 2001;888:248-255
37. Orakcioglu B, Uozumi Y, Kentar MM, Santos E, Unterberg A, Sakowitz OW. Evidence of spreading depolarizations in a porcine cortical intracerebral hemorrhage model. *Acta Neurochir Suppl*. 2012;114:369-372
38. Dreier JP, Major S, Pannek HW, Woitzik J, Scheel M, Wiesenthal D, Martus P, Winkler MK, Hartings JA, Fabricius M, Speckmann EJ, Gorji A, group Cs. Spreading convulsions, spreading depolarization and epileptogenesis in human cerebral cortex. *Brain*. 2012;135:259-275
39. Dreier JP, Woitzik J, Fabricius M, Bhatia R, Major S, Drenckhahn C, Lehmann TN, Sarrafzadeh A, Willumsen L, Hartings JA, Sakowitz OW, Seemann JH, Thieme A, Lauritzen M, Strong AJ. Delayed ischaemic neurological deficits after subarachnoid haemorrhage are associated with clusters of spreading depolarizations. *Brain*. 2006;129:3224-3237
40. Fabricius M, Fuhr S, Bhatia R, Boutelle M, Hashemi P, Strong AJ, Lauritzen M. Cortical spreading depression and peri-infarct depolarization in acutely injured human cerebral cortex. *Brain*. 2006;129:778-790
41. Hartings JA, Bullock MR, Okonkwo DO, Murray LS, Murray GD, Fabricius M, Maas AI, Woitzik J, Sakowitz O, Mathern B, Roozenbeek B, Lingsma H, Dreier JP, Puccio AM, Shutter LA, Pahl C, Strong AJ, Co-Operative Study on Brain Injury D. Spreading depolarisations and outcome after traumatic brain injury: A prospective observational study. *Lancet Neurol*. 2011;10:1058-1064
42. Helbok R, Schiefecker AJ, Friberg C, Beer R, Kofler M, Rhomberg P, Unterberger I, Gizewski E, Hauerberg J, Moller K, Lackner P, Broessner G, Pfausler B, Ortler M, Thome C, Schmutzhard E, Fabricius M. Spreading depolarizations in patients with spontaneous intracerebral hemorrhage: Association with perihematomal edema progression. *J Cereb Blood Flow Metab*. 2017;37:1871-1882
43. Oka F, Sadeghian H, Yaseen MA, Fu B, Kura S, Qin T, Sakadzic S, Sugimoto K, Inoue T, Ishihara H, Nomura S, Suzuki M, Ayata C. Intracranial pressure spikes trigger spreading depolarizations. *Brain*. 2022;145:194-207

44. Schiefecker AJ, Beer R, Pfausler B, Lackner P, Broessner G, Unterberger I, Sohm F, Mulino M, Thome C, Humpel C, Schmutzhard E, Helbok R. Clusters of cortical spreading depolarizations in a patient with intracerebral hemorrhage: A multimodal neuromonitoring study. *Neurocrit Care*. 2015;22:293-298
45. Schiefecker AJ, Kofler M, Gaasch M, Beer R, Unterberger I, Pfausler B, Broessner G, Lackner P, Rhomberg P, Gizewski E, Hackl WO, Mulino M, Ortler M, Thome C, Schmutzhard E, Helbok R. Brain temperature but not core temperature increases during spreading depolarizations in patients with spontaneous intracerebral hemorrhage. *J Cereb Blood Flow Metab*. 2018;38:549-558
46. Strong AJ, Fabricius M, Boutelle MG, Hibbins SJ, Hopwood SE, Jones R, Parkin MC, Lauritzen M. Spreading and synchronous depressions of cortical activity in acutely injured human brain. *Stroke*. 2002;33:2738-2743
47. Sugimoto K, Nomura S, Shirao S, Inoue T, Ishihara H, Kawano R, Kawano A, Oka F, Suehiro E, Sadahiro H, Shinoyama M, Oku T, Maruta Y, Hirayama Y, Hiyoshi K, Kiyohira M, Yoneda H, Okazaki K, Dreier JP, Suzuki M. Cilostazol decreases duration of spreading depolarization and spreading ischemia after aneurysmal subarachnoid hemorrhage. *Ann Neurol*. 2018;84:873-885
48. Woitzik J, Hecht N, Pinczolits A, Sandow N, Major S, Winkler MK, Weber-Carstens S, Dohmen C, Graf R, Strong AJ, Dreier JP, Vajkoczy P, group Cs. Propagation of cortical spreading depolarization in the human cortex after malignant stroke. *Neurology*. 2013;80:1095-1102
49. Kraig RP, Nicholson C. Extracellular ionic variations during spreading depression. *Neuroscience*. 1978;3:1045-1059
50. Takano T, Tian GF, Peng W, Lou N, Lovatt D, Hansen AJ, Kasischke KA, Nedergaard M. Cortical spreading depression causes and coincides with tissue hypoxia. *Nat Neurosci*. 2007;10:754-762
51. Chen SP, Ayata C. Spreading depression in primary and secondary headache disorders. *Curr Pain Headache Rep*. 2016;20:44
52. Andrew RD, Hartings JA, Ayata C, Brennan KC, Dawson-Scully KD, Farkas E, Herreras O, Kirov SA, Muller M, Ollen-Bittle N, Reiffurth C, Revah O, Robertson RM, Shuttleworth CW, Ullah G, Dreier JP. The critical role of spreading depolarizations in early brain injury: Consensus and contention. *Neurocrit Care*. 2022;37:83-101

53. Leao AA. Further observations on the spreading depression of activity in the cerebral cortex. *J Neurophysiol*. 1947;10:409-414
54. Matsuura T, Bures J. The minimum volume of depolarized neural tissue required for triggering cortical spreading depression in rat. *Exp Brain Res*. 1971;12:238-249
55. von Bornstadt D, Houben T, Seidel JL, Zheng Y, Dilekoz E, Qin T, Sandow N, Kura S, Eikermann-Haerter K, Endres M, Boas DA, Moskowitz MA, Lo EH, Dreier JP, Woitzik J, Sakadzic S, Ayata C. Supply-demand mismatch transients in susceptible peri-infarct hot zones explain the origins of spreading injury depolarizations. *Neuron*. 2015;85:1117-1131
56. Oka F, Hoffmann U, Lee JH, Shin HK, Chung DY, Yuzawa I, Chen SP, Atalay YB, Nozari A, Hopson KP, Qin T, Ayata C. Requisite ischemia for spreading depolarization occurrence after subarachnoid hemorrhage in rodents. *J Cereb Blood Flow Metab*. 2017;37:1829-1840
57. Hartings JA, York J, Carroll CP, Hinzman JM, Mahoney E, Krueger B, Winkler MKL, Major S, Horst V, Jahnke P, Woitzik J, Kola V, Du Y, Hagen M, Jiang J, Dreier JP. Subarachnoid blood acutely induces spreading depolarizations and early cortical infarction. *Brain*. 2017;140:2673-2690
58. Chung DY, Oka F, Ayata C. Spreading depolarizations: A therapeutic target against delayed cerebral ischemia after subarachnoid hemorrhage. *J Clin Neurophysiol*. 2016;33:196-202
59. Dreier JP, Ebert N, Priller J, Megow D, Lindauer U, Klee R, Reuter U, Imai Y, Einhaupl KM, Victorov I, Dirnagl U. Products of hemolysis in the subarachnoid space inducing spreading ischemia in the cortex and focal necrosis in rats: A model for delayed ischemic neurological deficits after subarachnoid hemorrhage? *J Neurosurg*. 2000;93:658-666
60. Dreier JP, Korner K, Ebert N, Gorner A, Rubin I, Back T, Lindauer U, Wolf T, Villringer A, Einhaupl KM, Lauritzen M, Dirnagl U. Nitric oxide scavenging by hemoglobin or nitric oxide synthase inhibition by n-nitro-l-arginine induces cortical spreading ischemia when k+ is increased in the subarachnoid space. *J Cereb Blood Flow Metab*. 1998;18:978-990
61. Petzold GC, Haack S, von Bohlen Und Halbach O, Priller J, Lehmann TN, Heinemann U, Dirnagl U, Dreier JP. Nitric oxide modulates spreading depolarization threshold in the human and rodent cortex. *Stroke*. 2008;39:1292-1299

62. Dohmen C, Sakowitz OW, Fabricius M, Bosche B, Reithmeier T, Ernestus RI, Brinker G, Dreier JP, Woitzik J, Strong AJ, Graf R, Co-Operative Study of Brain Injury D. Spreading depolarizations occur in human ischemic stroke with high incidence. *Ann Neurol*. 2008;63:720-728
63. Gursoy-Ozdemir Y, Qiu J, Matsuoka N, Bolay H, Bermpohl D, Jin H, Wang X, Rosenberg GA, Lo EH, Moskowitz MA. Cortical spreading depression activates and upregulates mmp-9. *J Clin Invest*. 2004;113:1447-1455
64. Grinberg YY, Dibbern ME, Levasseur VA, Kraig RP. Insulin-like growth factor-1 abrogates microglial oxidative stress and tnf-alpha responses to spreading depression. *J Neurochem*. 2013;126:662-672
65. Urbach A, Bruehl C, Witte OW. Microarray-based long-term detection of genes differentially expressed after cortical spreading depression. *Eur J Neurosci*. 2006;24:841-856
66. Takizawa T, Qin T, Lopes de Morais A, Sugimoto K, Chung JY, Morsett L, Mulder I, Fischer P, Suzuki T, Anzabi M, Bohm M, Qu WS, Yanagisawa T, Hickman S, Khoury JE, Whalen MJ, Harriott AM, Chung DY, Ayata C. Non-invasively triggered spreading depolarizations induce a rapid pro-inflammatory response in cerebral cortex. *J Cereb Blood Flow Metab*. 2020;40:1117-1131
67. Grinberg YY, Milton JG, Kraig RP. Spreading depression sends microglia on levy flights. *PLoS One*. 2011;6:e19294
68. Jander S, Schroeter M, Peters O, Witte OW, Stoll G. Cortical spreading depression induces proinflammatory cytokine gene expression in the rat brain. *J Cereb Blood Flow Metab*. 2001;21:218-225
69. Eikermann-Haerter K, Lee JH, Yuzawa I, Liu CH, Zhou Z, Shin HK, Zheng Y, Qin T, Kurth T, Waeber C, Ferrari MD, van den Maagdenberg AM, Moskowitz MA, Ayata C. Migraine mutations increase stroke vulnerability by facilitating ischemic depolarizations. *Circulation*. 2012;125:335-345
70. Risher WC, Ard D, Yuan J, Kirov SA. Recurrent spontaneous spreading depolarizations facilitate acute dendritic injury in the ischemic penumbra. *J Neurosci*. 2010;30:9859-9868
71. Sugimoto K, Shirao S, Koizumi H, Inoue T, Oka F, Maruta Y, Suehiro E, Sadahiro H, Oku T, Yoneda H, Ishihara H, Nomura S, Suzuki M. Continuous monitoring of spreading depolarization and cerebrovascular autoregulation after aneurysmal subarachnoid hemorrhage. *J Stroke Cerebrovasc Dis*. 2016;25:e171-177

72. Dreier JP, Major S, Manning A, Woitzik J, Drenckhahn C, Steinbrink J, Tolias C, Oliveira-Ferreira AI, Fabricius M, Hartings JA, Vajkoczy P, Lauritzen M, Dirnagl U, Bohner G, Strong AJ, group Cs. Cortical spreading ischaemia is a novel process involved in ischaemic damage in patients with aneurysmal subarachnoid haemorrhage. *Brain*. 2009;132:1866-1881
73. Hertle DN, Dreier JP, Woitzik J, Hartings JA, Bullock R, Okonkwo DO, Shutter LA, Vidgeon S, Strong AJ, Kowoll C, Dohmen C, Diedler J, Veltkamp R, Bruckner T, Unterberg AW, Sakowitz OW, Cooperative Study of Brain Injury D. Effect of analgesics and sedatives on the occurrence of spreading depolarizations accompanying acute brain injury. *Brain*. 2012;135:2390-2398
74. Santos E, Olivares-Rivera A, Major S, Sanchez-Porras R, Uhlmann L, Kunzmann K, Zerelles R, Kentar M, Kola V, Aguilera AH, Herrera MG, Lemale CL, Woitzik J, Hartings JA, Sakowitz OW, Unterberg AW, Dreier JP. Lasting s-ketamine block of spreading depolarizations in subarachnoid hemorrhage: A retrospective cohort study. *Crit Care*. 2019;23:427
75. Carlson AP, Abbas M, Alunday RL, Qeadan F, Shuttleworth CW. Spreading depolarization in acute brain injury inhibited by ketamine: A prospective, randomized, multiple crossover trial. *J Neurosurg*. 2018:1-7
76. Fischer P, Sugimoto K, Chung DY, Tamim I, Morais A, Takizawa T, Qin T, Gomez CA, Schlunk F, Endres M, Yaseen MA, Sakadzic S, Ayata C. Rapid hematoma growth triggers spreading depolarizations in experimental intracortical hemorrhage. *J Cereb Blood Flow Metab*. 2021;41:1264-1276
77. Umegaki M, Sanada Y, Waerzeggers Y, Rosner G, Yoshimine T, Heiss WD, Graf R. Peri-infarct depolarizations reveal penumbra-like conditions in striatum. *J Neurosci*. 2005;25:1387-1394
78. James ML, Warner DS, Laskowitz DT. Preclinical models of intracerebral hemorrhage: A translational perspective. *Neurocrit Care*. 2008;9:139-152
79. Manaenko A, Chen H, Zhang JH, Tang J. Comparison of different preclinical models of intracerebral hemorrhage. *Acta Neurochir Suppl*. 2011;111:9-14
80. Rosenberg GA, Mun-Bryce S, Wesley M, Kornfeld M. Collagenase-induced intracerebral hemorrhage in rats. *Stroke*. 1990;21:801-807
81. Chung DY, Sugimoto K, Fischer P, Bohm M, Takizawa T, Sadeghian H, Morais A, Harriott A, Oka F, Qin T, Henninger N, Yaseen MA, Sakadzic S, Ayata C. Real-

time non-invasive in vivo visible light detection of cortical spreading depolarizations in mice. *J Neurosci Methods*. 2018;309:143-146

82. Ayata C, Dunn AK, Gursoy OY, Huang Z, Boas DA, Moskowitz MA. Laser speckle flowmetry for the study of cerebrovascular physiology in normal and ischemic mouse cortex. *J Cereb Blood Flow Metab*. 2004;24:744-755
83. Dunn AK, Bolay H, Moskowitz MA, Boas DA. Dynamic imaging of cerebral blood flow using laser speckle. *J Cereb Blood Flow Metab*. 2001;21:195-201
84. Briers JD. Laser doppler, speckle and related techniques for blood perfusion mapping and imaging. *Physiol Meas*. 2001;22:R35-66
85. Foerch C, Arai K, Jin G, Park KP, Pallast S, van Leyen K, Lo EH. Experimental model of warfarin-associated intracerebral hemorrhage. *Stroke*. 2008;39:3397-3404
86. Feldman AT, Wolfe D. Tissue processing and hematoxylin and eosin staining. *Methods Mol Biol*. 2014;1180:31-43
87. Eikermann-Haerter K, Lee JH, Yalcin N, Yu ES, Daneshmand A, Wei Y, Zheng Y, Can A, Sengul B, Ferrari MD, van den Maagdenberg AM, Ayata C. Migraine prophylaxis, ischemic depolarizations, and stroke outcomes in mice. *Stroke*. 2015;46:229-236
88. Shin HK, Dunn AK, Jones PB, Boas DA, Lo EH, Moskowitz MA, Ayata C. Normobaric hyperoxia improves cerebral blood flow and oxygenation, and inhibits peri-infarct depolarizations in experimental focal ischaemia. *Brain*. 2007;130:1631-1642
89. Shin HK, Dunn AK, Jones PB, Boas DA, Moskowitz MA, Ayata C. Vasoconstrictive neurovascular coupling during focal ischemic depolarizations. *J Cereb Blood Flow Metab*. 2006;26:1018-1030
90. Addae JI, Stone TW. Effects of topically applied excitatory amino acids on evoked potentials and single cell activity in rat cerebral cortex. *Eur J Pharmacol*. 1986;121:337-343
91. Iliff JJ, D'Ambrosio R, Ngai AC, Winn HR. Adenosine receptors mediate glutamate-evoked arteriolar dilation in the rat cerebral cortex. *Am J Physiol Heart Circ Physiol*. 2003;284:H1631-1637
92. Woody CD. Glutamate induces different neuronal conditioned responses than acpd when used as a locally ionophoresed unconditioned stimulus in the cat motor cortex. *Physiol Res*. 2002;51 Suppl 1:S77-84

93. Hubschmann OR, Kornhauser D. Cortical cellular response in acute subarachnoid hemorrhage. *J Neurosurg*. 1980;52:456-462
94. Dang G, Yang Y, Wu G, Hua Y, Keep RF, Xi G. Early erythrolysis in the hematoma after experimental intracerebral hemorrhage. *Transl Stroke Res*. 2017;8:174-182
95. Aronowski J, Zhao X. Molecular pathophysiology of cerebral hemorrhage: Secondary brain injury. *Stroke*. 2011;42:1781-1786
96. Qing WG, Dong YQ, Ping TQ, Lai LG, Fang LD, Min HW, Xia L, Heng PY. Brain edema after intracerebral hemorrhage in rats: The role of iron overload and aquaporin 4. *J Neurosurg*. 2009;110:462-468
97. Thiex R, Tsirka SE. Brain edema after intracerebral hemorrhage: Mechanisms, treatment options, management strategies, and operative indications. *Neurosurg Focus*. 2007;22:E6
98. Wagner KR, Sharp FR, Ardizzone TD, Lu A, Clark JF. Heme and iron metabolism: Role in cerebral hemorrhage. *J Cereb Blood Flow Metab*. 2003;23:629-652
99. Elijovich L, Patel PV, Hemphill JC, 3rd. Intracerebral hemorrhage. *Semin Neurol*. 2008;28:657-667
100. Shin HK, Nishimura M, Jones PB, Ay H, Boas DA, Moskowitz MA, Ayata C. Mild induced hypertension improves blood flow and oxygen metabolism in transient focal cerebral ischemia. *Stroke*. 2008;39:1548-1555
101. Schlunk F, Bohm M, Boulouis G, Qin T, Arbel M, Tamim I, Fischer P, Bacskai BJ, Frosch MP, Endres M, Greenberg SM, Ayata C. Secondary bleeding during acute experimental intracerebral hemorrhage. *Stroke*. 2019;50:1210-1215
102. Chen Y, Chen S, Chang J, Wei J, Feng M, Wang R. Perihematomal edema after intracerebral hemorrhage: An update on pathogenesis, risk factors, and therapeutic advances. *Front Immunol*. 2021;12:740632
103. Enzmann DR, Britt RH, Lyons BE, Buxton JL, Wilson DA. Natural history of experimental intracerebral hemorrhage: Sonography, computed tomography and neuropathology. *AJNR Am J Neuroradiol*. 1981;2:517-526
104. Ironside N, Chen CJ, Ding D, Mayer SA, Connolly ES, Jr. Perihematomal edema after spontaneous intracerebral hemorrhage. *Stroke*. 2019;50:1626-1633
105. Barratt HE, Lanman TA, Carmichael ST. Mouse intracerebral hemorrhage models produce different degrees of initial and delayed damage, axonal sprouting, and recovery. *J Cereb Blood Flow Metab*. 2014;34:1463-1471

106. MacLellan CL, Silasi G, Poon CC, Edmundson CL, Buist R, Peeling J, Colbourne F. Intracerebral hemorrhage models in rat: Comparing collagenase to blood infusion. *J Cereb Blood Flow Metab*. 2008;28:516-525

107. Charidimou A, Boulouis G, Gurol ME, Ayata C, Bacskai BJ, Frosch MP, Viswanathan A, Greenberg SM. Emerging concepts in sporadic cerebral amyloid angiopathy. *Brain*. 2017;140:1829-1850

108. Charidimou A, Peeters A, Fox Z, Gregoire SM, Vandermeeren Y, Laloux P, Jager HR, Baron JC, Werring DJ. Spectrum of transient focal neurological episodes in cerebral amyloid angiopathy: Multicentre magnetic resonance imaging cohort study and meta-analysis. *Stroke*. 2012;43:2324-2330

109. Robinson D, Hartings J, Foreman B. First report of spreading depolarization correlates on scalp eeg confirmed with a depth electrode. *Neurocrit Care*. 2021;35:100-104

Eidesstattliche Versicherung

„Ich, Paul Fischer, versichere an Eides statt durch meine eigenhändige Unterschrift, dass ich die vorgelegte Dissertation mit dem Thema: Entstehungsmechanismen von Spreading Depolarizations in einem Mausmodell akuter und subakuter kortikaler Blutungen/ Mechanisms triggering spreading depolarizations in a mouse model of acute and subacute cortical hemorrhage selbstständig und ohne nicht offengelegte Hilfe Dritter verfasst und keine anderen als die angegebenen Quellen und Hilfsmittel genutzt habe.

Alle Stellen, die wörtlich oder dem Sinne nach auf Publikationen oder Vorträgen anderer Autoren/innen beruhen, sind als solche in korrekter Zitierung kenntlich gemacht. Die Abschnitte zu Methodik (insbesondere praktische Arbeiten, Laborbestimmungen, statistische Aufarbeitung) und Resultaten (insbesondere Abbildungen, Graphiken und Tabellen) werden von mir verantwortet.

Ich versichere ferner, dass ich die in Zusammenarbeit mit anderen Personen generierten Daten, Datenauswertungen und Schlussfolgerungen korrekt gekennzeichnet und meinen eigenen Beitrag sowie die Beiträge anderer Personen korrekt kenntlich gemacht habe (siehe Anteilserklärung). Texte oder Textteile, die gemeinsam mit anderen erstellt oder verwendet wurden, habe ich korrekt kenntlich gemacht.

Meine Anteile an etwaigen Publikationen zu dieser Dissertation entsprechen denen, die in der untenstehenden gemeinsamen Erklärung mit dem/der Erstbetreuer/in, angegeben sind. Für sämtliche im Rahmen der Dissertation entstandenen Publikationen wurden die Richtlinien des ICMJE (International Committee of Medical Journal Editors; www.icmje.og) zur Autorenschaft eingehalten. Ich erkläre ferner, dass ich mich zur Einhaltung der Satzung der Charité – Universitätsmedizin Berlin zur Sicherung Guter Wissenschaftlicher Praxis verpflichte.

Weiterhin versichere ich, dass ich diese Dissertation weder in gleicher noch in ähnlicher Form bereits an einer anderen Fakultät eingereicht habe.

Die Bedeutung dieser eidesstattlichen Versicherung und die strafrechtlichen Folgen einer unwahren eidesstattlichen Versicherung (§§156, 161 des Strafgesetzbuches) sind mir bekannt und bewusst.“

Anteilserklärung an der erfolgten Publikation

Publikation 1:
Fischer P, Sugimoto K, Chung DY, Tamim I, Morais A, Takizawa T, et al. Rapid hematoma growth triggers spreading depolarizations in experimental intracortical hemorrhage. J Cereb Blood Flow Metab. 2021

- Eigenständige Etablierung eines Modells zur Induktion einer rein intrakortikalen Blutung in der Maus auf Grundlage des zuvor erlernten striatalen Blutungsmodells und einer strukturierten Literaturrecherche
- Eigenständige Etablierung der simultanen Nutzung von Elektrokortikographie, Laser Speckle Flowmetry (LSF) und Intrinsic Optical Signaling (IOS) während einer experimentellen intrakortikalen Blutung in der Maus
- Selbständiges Design, Durchführung und laufende Anpassung aller Experimente entsprechend der Zwischenergebnisse (Figures 1-7, Supplementary Figure 1, Supplementary Table 1, Supplementary Movies 1-2)
    - Zwei experimentelle Prozeduren wurden nach meiner Planung durch andere Mitglieder der Gruppe durchgeführt: die Operation zur distalen MCAo durch Kazutaka Sugimoto (Fig.7), die Glutamat- und Aspartat-Injektionen durch Andreia Morais (Daten nicht gezeigt)
- Eigenständige Datenanalyse der Blutungsgröße im zeitlichen Verlauf (IOS Bilder), des Auftretens von kortikalen Spreading Depolarizations im Elektrokortikogramm (Labchart) und des zerebralen Blutflusses mittels Laser Speckle Flowmetry (Matlab) sowie anschließende Analyse des Hirngewebes (Figures 1-7, Supplementary Figure 1, Supplementary Table 1, Supplementary Movies 1-2)
    - Einzig die Erstellung des Matlab-Skriptes zur Umwandlung der LSF-Bilder erfolgte durch ein anderes Gruppenmitglied, David Chung (Fig.1, Fig.4)
- Statistische Auswertung und Visualisierung der Daten (eigenständiges Erstellen der Figures 1-7; Supplementary Figure 1,Table 1, Movies 1-2)
- Selbständiger Entwurf und Einreichen des Manuskriptes, Adressierung der Kommentare der Reviewer (in enger Rücksprache mit Prof. Cenk Ayata)
- Vorstellung der Arbeit auf wissenschaftlicher Kongressen

Journal Summary List

Journal Data Filtered By: **Selected JCR Year: 2018** Selected Editions: SCIE,SSCI
Selected Categories: **"NEUROSCIENCES"** Selected Category Scheme: WoS
Gesamtanzahl: 267 Journale

Rank	Full Journal Title	Total Cites	Journal Impact Factor	Eigenfactor Score
1	NATURE REVIEWS NEUROSCIENCE	43,107	33.162	0.068480
2	NATURE NEUROSCIENCE	63,390	21.126	0.164700
3	ACTA NEUROPATHOLOGICA	20,206	18.174	0.041660
4	BEHAVIORAL AND BRAIN SCIENCES	9,377	17.194	0.010240
5	TRENDS IN COGNITIVE SCIENCES	27,095	16.173	0.040040
6	JOURNAL OF PINEAL RESEARCH	10,695	15.221	0.010560
7	NEURON	95,348	14.403	0.218680
8	TRENDS IN NEUROSCIENCES	20,163	12.314	0.024480
9	Annual Review of Neuroscience	14,042	12.043	0.015020
10	MOLECULAR PSYCHIATRY	20,353	11.973	0.049290
11	BRAIN	52,970	11.814	0.074030
12	BIOLOGICAL PSYCHIATRY	43,122	11.501	0.053320
13	PROGRESS IN NEUROBIOLOGY	12,929	10.658	0.013230
14	Nature Human Behaviour	1,230	10.575	0.006550
15	SLEEP MEDICINE REVIEWS	6,920	10.517	0.010920
16	ANNALS OF NEUROLOGY	37,336	9.496	0.048630
17	Molecular Neurodegeneration	4,248	8.274	0.011350
18	NEUROSCIENCE AND BIOBEHAVIORAL REVIEWS	26,724	8.002	0.051580
19	FRONTIERS IN NEUROENDOCRINOLOGY	4,196	7.852	0.005490
20	Neurology-Neuroimmunology & Neuroinflammation	1,996	7.353	0.008220
21	NEUROPSYCHOPHARMACOLOGY	25,672	7.160	0.039090

Rank	Full Journal Title	Total Cites	Journal Impact Factor	Eigenfactor Score
22	Brain Stimulation	5,457	6.919	0.014470
23	NEUROPATHOLOGY AND APPLIED NEUROBIOLOGY	3,876	6.878	0.006420
24	NEUROENDOCRINOLOGY	5,046	6.804	0.005690
25	NEUROSCIENTIST	4,986	6.791	0.008520
26	BRAIN BEHAVIOR AND IMMUNITY	14,533	6.170	0.025700
27	BRAIN PATHOLOGY	5,263	6.155	0.007880
28	Alzheimers Research & Therapy	3,160	6.142	0.010700
29	JOURNAL OF NEUROSCIENCE	175,046	6.074	0.233460
30	JOURNAL OF CEREBRAL BLOOD FLOW AND METABOLISM	19,766	6.040	0.028050
31	PAIN	38,312	6.029	0.039070
32	CURRENT OPINION IN NEUROBIOLOGY	15,090	6.014	0.033650
33	Acta Neuropathologica Communications	3,063	5.883	0.014190
34	Translational Stroke Research	1,955	5.847	0.004330
35	GLIA	14,003	5.829	0.018760
36	NEUROIMAGE	99,720	5.812	0.132720
37	NEURAL NETWORKS	13,063	5.785	0.016060
38	NEUROPSYCHOLOGY REVIEW	2,971	5.739	0.003940
39	Molecular Autism	2,107	5.712	0.008000
40	Journal of Neuroinflammation	11,767	5.700	0.023240
41	Multiple Sclerosis Journal	11,501	5.649	0.022750
42	Annual Review of Vision Science	458	5.622	0.003300
43	Neurotherapeutics	4,475	5.552	0.009060
44	Translational Neurodegeneration	810	5.534	0.002420

Selected JCR Year: 2018; Selected Categories: “NEUROSCIENCES”

Druckexemplar der Publikation

https://doi.org/10.1177/0271678X20951993

Lebenslauf

Mein Lebenslauf wird aus datenschutzrechtlichen Gründen in der elektronischen Version meiner Arbeit nicht veröffentlicht.

Pubilkationsliste

1. **Fischer P**, Tamim I, Sugimoto K, Morais A, Takizawa T, Qin T, Schlunk F, Endres M, Yaseen MA, Chung DY, Sakadžić S, Ayata C. Spreading depolarizations suppress hematoma growth in hyperacute intracerebral hemorrhage in mice. *Under Review*

2. Sugimoto K, Yang J, **Fischer P**, Takizawa T, Mulder I, Qin T, Erdogan T, Yaseen MA, Sakadžić S, Chung DY, Ayata C. Optogenetic spreading depolarizations do not worsen acute ischemic stroke outcome. Stroke. 2023; 54(4):1110-1119

   Impact factor: 10.17

3. Schlunk F*, **Fischer P***, Princen HMG, Rex A, Prinz V, Foddis M, Lutjohann D, Laufs U, Endres M. No effects of pcsk9-inhibitor treatment on spatial learning, locomotor activity, and novel object recognition in mice. Behav Brain Res. 2021;396:112875

   Impact factor: 3.33

4. **Fischer P**, Sugimoto K, Chung DY, Tamim I, Morais A, Takizawa T, Qin T, Gomez CA, Schlunk F, Endres M, Yaseen MA, Sakadzic S, Ayata C. Rapid hematoma growth triggers spreading depolarizations in experimental intracortical hemorrhage. J Cereb Blood Flow Metab. 2021;41:1264-1276

   Impact factor: 6.04

5. Takizawa T, Qin T, Lopes de Morais A, Sugimoto K, Chung JY, Morsett L, Mulder I, **Fischer P**, Suzuki T, Anzabi M, Bohm M, Qu WS, Yanagisawa T, Hickman S, Khoury JE, Whalen MJ, Harriott AM, Chung DY, Ayata C. Non-invasively triggered spreading depolarizations induce a rapid pro-inflammatory response in cerebral cortex. J Cereb Blood Flow Metab. 2020;40:1117-1131

   Impact factor: 6.04

6. Sugimoto K, Chung DY, Bohm M, **Fischer P**, Takizawa T, Aykan SA, Qin T, Yanagisawa T, Harriott A, Oka F, Yaseen MA, Sakadzic S, Ayata C. Peri-infarct hotzones have higher susceptibility to optogenetic functional activation-induced spreading depolarizations. Stroke. 2020;51:2526-2535

   Impact factor: 7.19

7. Schlunk F, **Fischer P**, Princen HMG, Rex A, Prinz V, Foddis M, Lutjohann D, Laufs U, Endres M. Effects of inhibition or deletion of pcsk9 (proprotein convertase subtilisin/kexin type 9) on intracerebral hemorrhage volumes in mice. Stroke. 2020;51:e297-e298

   Impact factor: 7.19

8. Schlunk F, Bohm M, Boulouis G, Qin T, Arbel M, Tamim I, **Fischer P**, Bacskai BJ, Frosch MP, Endres M, Greenberg SM, Ayata C. Secondary bleeding during acute experimental intracerebral hemorrhage. Stroke. 2019;50:1210-1215

   Impact factor: 6.05

9. Chung DY, Sugimoto K, **Fischer P**, Bohm M, Takizawa T, Sadeghian H, Morais A, Harriott A, Oka F, Qin T, Henninger N, Yaseen MA, Sakadzic S, Ayata C. Real-time non-invasive in vivo visible light detection of cortical spreading depolarizations in mice. J Neurosci Methods. 2018;309:143-146

   Impact factor: 2.67

10. Akhter M, Qin T, **Fischer P**, Sadeghian H, Kim HH, Whalen MJ, Goldstein JN, Ayata C. Rho-kinase inhibitors do not expand hematoma volume in acute experimental intracerebral hemorrhage. Ann Clin Transl Neurol. 2018;5:769-776

    Impact factor: 4.65

* geteilte Erstautorenschaft

Danksagung

Mein tiefster Dank gebührt Prof. Cenk Ayata meinem Supervisor und Gruppenleiter in der Neurovascular Research Unit am Massachusetts General Hospital und der Harvard Medical School. Seine Leidenschaft für die Forschung, fundierte Expertise und hervorragende Lehre und Betreuung, haben meine Entwicklung als junger Wissenschaftler nachhaltig geprägt und werden dies auch in Zukunft tun. Ohne seine Supervision wäre diese Arbeit, die im stetigen kritischen Diskurs mit ihm entstand, nicht zustande gekommen.

Gleichermaßen möchte ich meinem Doktorvater Prof. Dr. Matthias Endres danken, ohne dessen Vertrauen und Unterstützung ich den Forschungsaufenthalt am Massachusetts General Hospital und der Harvard Medical School nicht hätte realisieren können. Sein Mentoring und die mir zuteil werdende Förderung in seiner Arbeitsgruppe haben den erfolgreichen Abschluss meiner Arbeit erst ermöglicht und unterstützen mich weiterhin entscheidend in meiner wissenschaftlichen Laufbahn.

Ich danke weiterhin Dr. Frieder Schlunk, der mir die Grundlagen experimentellen Arbeitens und ein breites Spektrum an Fähigkeiten in den Laboren der experimentellen Neurologie vermittelt hat. Seine ausgezeichnete Betreuung und sein Enthusiasmus haben meine Begeisterung für die Forschung an intrazerebralen Blutungen geweckt und den Grundstein für eigenständiges Arbeiten gelegt. Insbesondere während der ersten Monate meiner Arbeit in Boston war er ein wichtiger Rückhalt.

Die Mitglieder der Neurovascular Research Unit haben die Arbeit an meiner Promotion zu einer Erfahrung gemacht, auf die ich immer mit Freude zurückblicken werde. Ihre Kritik, Fragen und Ideen halfen mir meine Arbeit im Verlauf immer wieder aus verschiedenen Blickwinkeln zu hinterfragen. Die Zusammenarbeit mit ihnen habe ich auf persönlicher wie fachlicher Ebene stets als bereichernd empfunden.

Zuletzt möchte ich meinen Eltern, meinem Bruder und Mira danken. Unzählige Stunden haben sie mit Korrekturlesen und Beratung zur graphischen Gestaltung und dem inhaltlichen Aufbau meiner Arbeiten verbracht. Vor allem aber konnte ich mich bei Rückschlägen infolge missglückter Experimente oder erfolgloser Bewerbungen immer auf ihren Rückhalt verlassen.